WIRELESS ENGINEER

Vol. XXV JULY 1948 No. 298

Standard Terms and Abbreviations

IN our May issue we published two letters referring to the March editorial on the above subject. In both letters reference was made to the abbreviation db for decibel. The standard abbreviation for the ampere is A, for the volt V, and for the watt W, and one might therefore expect the abbreviation for the bel to be B and for the neper N, but in the Glossary of Terms used in Telecommunication, British Standard 204 of 1943, the abbreviations for the decibel and decineper are given as db and dn. This was also the case in the 1936 Glossary, so it is not surprising that Mr. Odell has noticed "reference being made to a symbol—db." One cannot be dogmatic in such matters; the abbreviation for the metre is m not M, and for the gramme g not G. Mr. Odell says "if the db is considered *de rigueur*, we shall be expected to assimilate other horrors without protest." He is obviously unaware that db is the universally recognised usage, found in all the publications of the G.P.O., Bell Telephone Laboratories, etc., and he will certainly be expected to swallow such horrors as cm and kg. We agree, however, that there is a slight inconsistency in the treatment of the two Scots, Bell and Napier, as compared with that of Ampère, Volta, Ohm, and Faraday, but not such as to cause their shades to lodge a protest. The cases are peculiar in that b and n have not been adopted as abbreviations of bel and neper, as these are rarely used; the abbreviations are only for the decibel and decineper. In the Glossary no abbreviations are suggested for bel and neper, so that if ever they do occur they should be written in full.

We have referred on previous occasions to the point raised by Mr. Hart as to the relative merits of k and K as the abbreviation of kilo, but we disagree entirely with his suggestion that the advantages of the capital letter are so obvious that scientific journals should adopt it with the object of forcing the hand of the international standards organisation. The only thing in favour of the capital K is that it would be easier for people who are vague or careless about such things to remember that a million is M and not m if all sub-multiples of unity were represented by small letters and all multiples by capitals. The kilo is, however, not peculiar to electrical engineering; kilogrammes and kilometres occur in other branches of engineering and enter into the daily life of people in all metric countries. If a change were made it would have to be by international agreement. It is surely not very difficult to remember, if it has once been impressed on one, that mega is the only decimal prefix with a capital abbreviation.

If one looks up the literature of fifty years ago, one finds a tendency to avoid abbreviations; even such words as kilogrammes are printed over and over again in full in some textbooks. Where "kilowatts" was abbreviated it was usually KW even if km and kg occurred in the same line. An exception was Hobart's "Heavy Electrical Engineering" of 1908 in which he consistently wrote kw and kva, and expressed coal consumption in kg per kw hr or kg per hp hr. By adopting k as the recommended abbreviation the standardizing authorities brought electrical engineering usage into line with the universally adopted kg and km, and one has now become so used to kW that KW cries aloud for correction.

The only, but sufficient, reason for adopting the capital M for mega and the greek μ for micro was the fact that m was universally used for milli. There is no such reason for adopting the capital K for kilo, and the small k is as firmly entrenched in kg and km as is the small m in mm. We have recently looked through current numbers of electrical journals published in France, Switzerland, Holland and Germany and we were agreeably surprised to find that, without a single exception, the standard symbols and abbreviations were used with meticulous care. The consistent use of kW and kVA is the more noteworthy in countries like Germany where all nouns — including Kilogrammes — are written with a capital letter.

G. W. O. H.

GEOMETRY OF RECTANGULAR WAVEGUIDES

By A. C. Bartlett, M.A., Sc.D.

1. Introduction

THE purpose of this article is to point out some very simple geometrical properties of rectangular waveguides which lie hidden in the standard formulae and equations.

As a preliminary it is necessary to recall two simple theorems in geometry which will be used a number of times.

Theorem I.

If ABC is a triangle in which A is a right angle and AN is the perpendicular from A to BC then—

$$\frac{1}{AN^2} = \frac{1}{AB^2} + \frac{1}{AC^2}$$

Theorem II.

If ABCD is a tetrahedron in which the three angles BAC, CAD and DAB at the vertex A are right angles, and AN is the perpendicular from A to the face BCD then—

$$\frac{1}{AN^2} = \frac{1}{AB^2} + \frac{1}{AC^2} + \frac{1}{AD^2}$$

It is also necessary to discuss briefly some of the types of plane electromagnetic waves. All textbooks describe one type of plane wave which will be afterwards called the "standard plane wave." This wave has the property that adjacent equiphase planes are separated by a distance λ, the wavelength; that if f is the frequency—

$$\lambda \times f = c = 3 \times 10^{10} \text{ cm/sec}$$
$$= \text{the velocity of light.}$$

It has also the property that the electric and magnetic vectors are at right angles one to another and to the direction of propagation, and are everywhere the same in magnitude and direction. But if we define a plane wave simply as a wave having parallel planes of equal phase, the "standard plane wave" is not the only plane wave. The wave in a concentric transmission line is a plane wave differing from the standard plane wave in that the electric and magnetic vectors vary in magnitude and direction over the equiphase planes. Again the wave that occurs in straight tubular waveguides is also a plane wave differing from the standard plane wave in a number of respects :—

(1) The distance between adjacent equiphase planes (i.e., the wavelength λ_t) is always greater than λ of the standard plane wave of the same frequency. Hence the phase velocity $f \times \lambda_t$ is always greater than the velocity of light.

(2) The electric and magnetic vectors are not confined to the equiphase planes but one or both have components perpendicular to these planes.

(3) The magnitude of the vectors varies in a complicated pattern over the equiphase planes.

Another type of plane wave, to be treated in Sect. 7, has a wavelength λ_p which is less than λ; thus its phase velocity is always less than the velocity of light, and can be even less than a snail's pace. This wave has an axis of exponential attenuation at right angles to the phase propagation axis. It will be called the "simple plane attenuated wave."

Finally, it must be emphasized that when λ is used in this article without a subscript it will always refer to the wavelength of a

MS accepted by the Editor March, 1947.

standard plane wave in vacuum and can be converted into frequency by the relation $\lambda f = c$.

2. Rectangular Waveguides

It is well known that a waveguide will transmit energy freely in any mode if λ is sufficiently small; this will be known as the Transmitting Case. For each mode however there is a critical length dependent on the dimensions of the tube, and if λ is greater than this, energy is no longer freely transmitted, but is strongly reflected and there is an exponential attenuation of intensity along the tube; this Attenuating Case will be treated later in Sect. 6.

In the Transmitting Case it is known that the field of the plane wave in the guide is identical with the combined fields of four

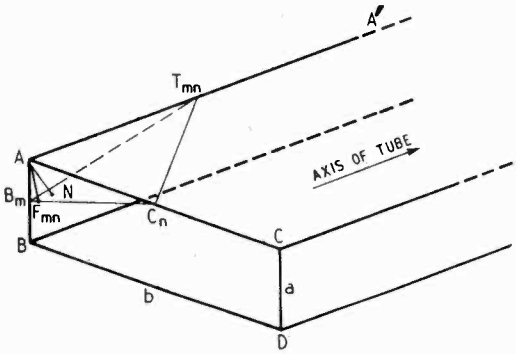

Fig. 1. *Rectangular waveguide; m and n are both taken to be 2.*

standard plane waves. In the Attenuating Case the field in the guide is identical with the combined fields of four simple plane attenuated waves. There is an apparent exception in the case of H_{0n} and H_{m0} modes which require only two standard plane waves, but this is merely because the four waves coalesce by pairs into two; the H_{0n} and H_{m0} modes are dealt with in Sect. 8.

3. Geometry of the Transmitting Case

Consider a rectangular waveguide as shown in Fig. 1, the lengths AB and AC of the cross-section being a and b respectively and suppose that an mn-wave (either H or E) is being propagated along the tube. From a standard formula* we know that λ_t the wavelength along the tube is determined by

$$\frac{1}{\lambda_t^2} = \frac{1}{\lambda^2} - \left(\frac{m}{2a}\right)^2 - \left(\frac{n}{2b}\right)^2$$

* Lamont—"Wave-Guides"—Methuen, p. 7.

which can be rewritten as

$$\frac{1}{(\lambda/2)^2} = \frac{1}{(\lambda_t/2)^2} + \frac{1}{(a/m)^2} + \frac{1}{(b/n)^2} \quad \ldots \quad (1)$$

Carry out now the following geometrical construction; in Fig. 1 take a point B_m in AB such that $AB_m = AB/m$ and a point C_n in AC such that $AC_n = AC/n$. Construct a sphere of radius $\lambda/2$ with centre A; rotate a plane about the line B_mC_n till it touches the sphere in a point N and let it cut the edge AA' in the point T_{mn}.

Consider now the tetrahedron $AB_mC_nT_{mn}$; all three angles at A are at right angles, and AN is the perpendicular from A to $B_mC_nT_{mn}$; we can therefore apply Theorem II, obtaining

$$\frac{1}{AN^2} = \frac{1}{AT_{mn}^2} + \frac{1}{AB_m^2} + \frac{1}{AC_n^2}$$

$$\text{i.e.,} \quad \frac{1}{(\lambda/2)^2} = \frac{1}{AT_{mn}^2} + \frac{1}{(a/m)^2} + \frac{1}{(b/n)^2}$$

Comparing this with Equation 1 we see that

$$AT_{mn} = \lambda_t/2$$

Thus we have arrived at a simple geometrical construction for λ_t. The construction of the sphere is not easy in practice, though it can often be carried out by eye sufficiently well to afford a useful estimate of the value of λ_t. But fortunately the operation can, without difficulty, be broken up into two plane diagrams. In Fig. 1, drop a perpendicular AF_{mn} from A to B_mC_n, and let its length be d_{mn}.

Then applying Theorem I

$$\frac{1}{AF_{mn}^2} = \frac{1}{AB_m^2} + \frac{1}{AC_n^2}$$

$$\text{i.e.,} \quad \frac{1}{d_{mn}^2} = \frac{1}{(a/m)^2} + \frac{1}{(b/n)^2}$$

With the help of this formula we can now write Equ. (1) as—

$$\frac{1}{(\lambda/2)^2} = \frac{1}{(\lambda_t/2)^2} + \frac{1}{d_{mn}^2} \quad \ldots \quad \ldots \quad (2)$$

and again using Theorem I we can construct

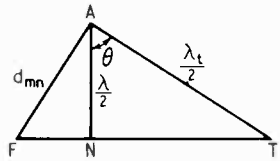

Fig. 2. *Determination of λ_t.*

a triangle AFT as shown in Fig. 2, with a right angle at A, $AN = \lambda/2$, and $AF = d_{mn}$, so that $AT = \lambda_t/2$. This triangle which determines λ_t simply and easily is very

instructive and in Fig. 3 are drawn two cases for the same d_{mn}, one in which λ/d_{mn} is small, the other where $\lambda/2$ is approaching equality with d_{mn}.

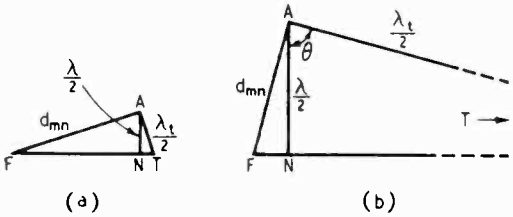

Fig. 3. *In both triangles d_{mn} is the same, but in (a) λ/d_{mn} is small and in (b) it is large.*

We see at once that λ_t is always greater than λ; that when λ is small, λ_t is only fractionally greater than λ, but as $\lambda/2$ increases and approaches d_{mn}, λ_t approaches infinity. When $\lambda/2 > d_{mn}$ the construction fails and we are in the presence of the Attenuating Case the geometry of which is dealt with later in Sect. 7.

In passing it should be noticed that the triangles AFT of Fig. 2 and $AF_{mn}T_{mn}$ of Fig. 1 are one and the same.

The significance of the plane $B_mC_nT_{mn}$ of Fig. 1 is of importance. This plane is the equiphase plane, and AN is the direction of propagation, of one of the four standard plane waves whose combined field is identical with the waveguide field. Similar planes associated in like manner with the other three corners B, C and D determine the other three waves. If the electric vectors of the four plane waves are perpendicular to the axis of the tube we have an H wave, if the magnetic vectors are perpendicular to the axis an E wave.

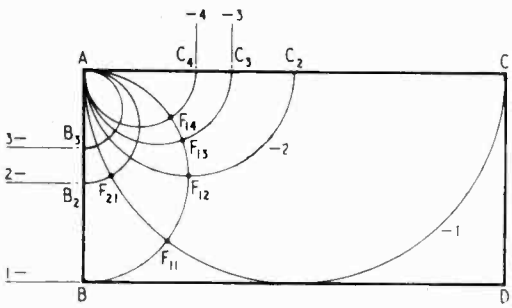

Fig. 4. *Geometrical construction for the points F_{mn} and the lengths $d_{mn} = AF_{mn}$.*

The angle θ that the axis of propagation of each of the four simple plane waves makes with the axis of the guide is the angle NAT_{mn} of Fig. 1 or the angle NAT of Figs. 2 and 3 and therefore—

$$\sin\theta = \frac{\lambda}{2d_{mn}}, \cos\theta = \frac{\lambda}{\lambda_t} \text{ and}$$

$$\tan\theta = \frac{\lambda_t}{2d_{mn}} \qquad \ldots \qquad \ldots \quad (3)$$

The verification that the combined fields of these four simple plane waves is the same as the waveguide field is easy and can be left to the reader.

4. Critical Wavelengths

We have seen that the critical wavelength for any mode mn is equal to $2d_{mn}$ and it is of interest to determine the set of lengths d_{mn}. It is easily done by the following construction. In the rectangle ABCD of Fig. 4, a transverse section of the guide,

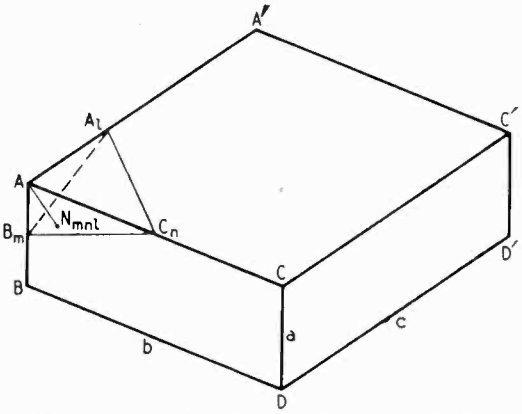

Fig. 5. *Construction for natural wavelength of a rectangular box resonator; m and n are taken as 2 and l as 3.*

draw a set of semicircles on AB, AB_2, AB_3, etc. as diameters and label them 1—, 2—, 3—, etc. respectively; on AC, AC_2, AC_3, etc., as diameters draw further semicircles and label tham —1, —2, —3, etc. It is easily proved then that the point of intersection of the semicircle m— and the semicircle —n is the point F_{mn}. If for any λ we draw a circle radius $\lambda/2$ with centre A then every mode whose F_{mn} lies without this circle will be a transmitting mode; every F_{mn} within the circle will be attended by an attenuating mode.

5. Resonant Wavelengths of a Rectangular Box

The resonant wavelengths of a rectangular box, such as is shown in Fig. 5, can be readily found by an application of the construction of Fig. 1. Let a, b and c be the lengths of the sides AB, AC, and AA′ respectively and let

the mode numbers corresponding to the sides AB, AC and AA′ be m, n and l. Take points A_l, B_m and C_n in AA′, AB and AC respectively so that

$$A_l = \frac{AA'}{l},\ B_m = \frac{AB}{m} \text{ and } AC_n = \frac{AC}{n}$$

Draw a perpendicular AN_{lmn} from A to the plane $A_lB_mC_n$. Then AN_{lmn} is obviously the resonant $\lambda/2$ for the lmn mode. The field pattern inside the resonator is the combined field of eight simple plane waves, one wave associated with each corner and each wave moving in a direction from outside to inside of the box.

The construction is three dimensional and not easy to carry out in practice, but again a useful guess can be made by eye. Take, for example a resonator of the same size as an ordinary match box—it can easily be seen that for the 111 mode, AN_{111} is about 1.5 cm, therefore the resonant wavelength for this mode is about 3 cm and the resonant frequency $3 \times 10^{10} \div 3 = 10{,}000$ Mc/s. A simple practical way of determining AN_{lmn} is to take a rectangular block and a flat-bottomed bowl of water. The corner A of Fig. 5 is pressed against the bottom of the bowl; simultaneously the block is tilted about, and water either poured in or baled out until the condition is reached that A_l, B_m and C_n all three lie in the water surface; the depth of water is then $\lambda/2$ for the mode.

An accurate plane diagram can be made in the following way (Fig. 6). Take an axis AX and mark on it from Fig. 4 the set of lengths AF_{mn}; on each AF_{mn} as diameter describe a semicircle and mark it—mn. On an axis at right angles mark off the lengths AA′, AA_2, AA_3 from Fig. 5 and on each of these construct a semicircle marking them 1—, 2—, 3— and so on. The distance from A to the point G_{lmn} where the semicircle l— cuts the semicircle —mn is the length AN_{lmn}, the half-resonant wavelength for the mode lmn.

6. Attenuating Case

A necessary preliminary is to investigate some of the properties of the simple plane attenuated wave. The standard plane wave is obtained by seeking solutions of the wave equation

$$\frac{\delta^2 R}{\delta x^2} + \frac{\delta^2 R}{\delta y^2} + \frac{\delta^2 R}{\delta z^2} - \frac{1}{c^2}\frac{\delta^2 R}{\delta t^2} = 0$$

of the form exp. $\{j(\omega t - ax - by - cz)\}$. The new type of wave is obtained by seeking solutions of the form exp. $\{j(\omega t - ax - by - cz) - \alpha z - \beta y - \gamma z\}$.

First consider the physical meaning of this type of solution—it can be written in the form

$$\exp.\ (j\omega t)\ \exp.\{-j(ax + by + cz)\}\ \exp.\ \{-(\alpha + \beta y + \gamma z)\}$$

and therefore over any plane $\alpha x + \beta y + \gamma z =$ constant, the amplitude is the same while over any plane $ax + by + cz =$ constant, the phase is the same. Hence we have two sets of parallel planes one set of equal amplitudes and the other of equal phase.

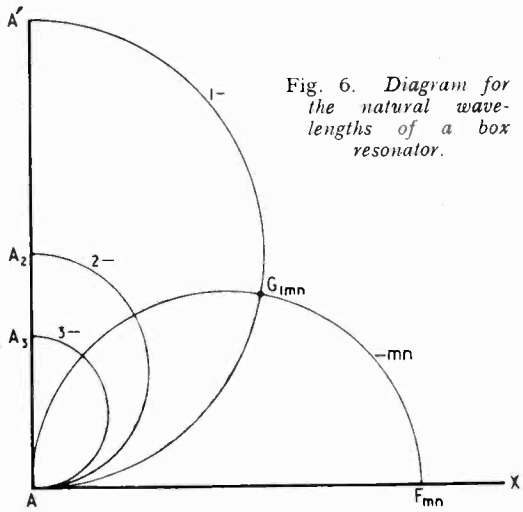

Fig. 6. *Diagram for the natural wavelengths of a box resonator.*

Performing the necessary double differentiations and substituting the results in the wave equation we obtain—

$$(ja + \alpha)^2 + (jb + \beta)^2 + (jc + \gamma)^2 + \left(\frac{2\pi}{\lambda}\right)^2 = 0,$$

and on separating real and imaginary parts—

$$(a^2 + b^2 + c^2) - (\alpha^2 + \beta^2 + \gamma^2) = \left(\frac{2\pi}{\lambda}\right)^2$$

and

$$a\alpha + b\beta + c\gamma = 0.$$

The second equation of the pair has an immediate interpretation—it is the standard condition that the planes $ax + by + cz =$ constant, and $\alpha x + \beta y + \gamma z =$ constant, are perpendicular to one another.

To interpret the first equation we consider the question of wavelength; the perpendicular from the origin to the plane $ax + by + cz =$ constant is $\dfrac{ax + by + cz}{\sqrt{a^2 + b^2 + c^2}}$ where x,

y and z are the co-ordinates of any point in the plane; this distance will be called h_1. There is a corresponding perpendicular $h_2 = \dfrac{\alpha x + \beta y + \gamma z}{\sqrt{\alpha^2 + \beta^2 + \gamma^2}}$ on to the plane $\alpha x + \beta y + \gamma z$ = constant and by using these expressions for h_1 and h_2 we can now write the exponential solution in the form—

$$\exp.\ (j\omega t)\ \exp.\ (-jh_1\sqrt{a^2 + b^2 + c^2})$$
$$\exp.\ (-h_2\sqrt{\alpha^2 + \beta^2 + \gamma^2})$$

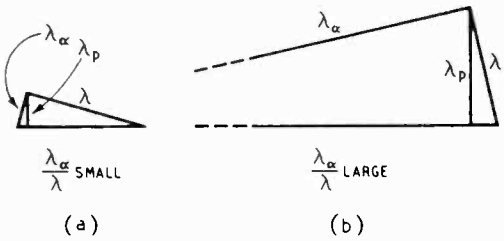

Fig. 7. *The relation between λ, λ_a and λ_p is shown here for λ_a/λ large (a) and small (b).*

Suppose now that h_1 is changed in length by an amount $2\pi/\sqrt{a^2 + b^2 + c^2}$, then the factor exp. $\{-jh_1\sqrt{a^2 + b^2 + c^2}\}$ is altered by a factor $e^{j2\pi}$ which is equivalent to a change of phase 2π; thus it follows that the wavelength, which will be denoted by λ_p is equal to $2\pi/\sqrt{a^2 + b^2 + c^2}$.

By a similar argument if we change h_2 by a length $2\pi/\sqrt{\alpha^2 + \beta^2 + \gamma^2}$ we pass to another plane of the $\alpha x + \beta y + \gamma z$ = constant, where the amplitude has diminished by a factor $e^{2\pi}$. This length $2\pi/\sqrt{\alpha^2 + \beta^2 + p^2}$ corresponding to a factor $e^{2\pi}$ in the same way that λ_p corresponds to a wavelength or $e^{j2\pi}$ will (for want of an accepted name), be termed the Attenuation Length and be denoted by λ_a.

The exponential solution takes now the form

$$e^{j\omega t} \cdot e^{-j\pi 2/\lambda_p} \cdot e^{-2\pi/\lambda_a}$$

while the equation

$$(a^2 + b^2 + c^2) - (\alpha^2 + \beta^2 + \gamma^2) = \left(\frac{2\pi}{\lambda}\right)^2$$

can be put in the form

$$\left(\frac{2\pi}{\lambda_p}\right)^2 - \left(\frac{2\pi}{\lambda_a}\right)^2 = \left(\frac{2\pi}{\lambda}\right)^2$$

or

$$\frac{1}{\lambda_p^2} = \frac{1}{\lambda^2} + \frac{1}{\lambda_a^2} \qquad \ldots \quad \ldots \quad \ldots \quad (4)$$

Theorem I can be applied to this relation between λ_p, λ_a and λ and we obtain the triangular construction of which two cases are shown in Fig. 7.

It is at once seen that λ_a can have any value, that $\lambda_p \not> \lambda$ and can have any value between o and λ. When λ_a is small λ_p is small, and when λ_a approaches infinity, λ_p approaches λ. The limiting case $\lambda_a = \infty$ and $\lambda_p = \lambda$ reduces to the standard plane wave.

It will be observed that λ_a enters into the problem as the peer of λ_p and therefore merits a name of its own, while $e^{2\pi}$ = 535·5 approx. seems to be the natural unit of attenuation.

The simple plane attenuated wave is of general importance and appears in several classical problems; in the theory of total internal reflection of light, a wave of this kind occurs in the less dense medium, its propagation axis being parallel to and its attenuation axis perpendicular to the inter-surface; the existence of this wave has been demonstrated experimentally. Again it appears in Zenneck's† famous treatment of the propagation of electromagnetic waves over the surface of a flat dissipative earth.

The Zenneck case is that of the refraction of such a wave at the surface of a denser dissipative medium with λ_p, λ_a and the angle of incidence chosen so that there is no reflected wave, a more recondite case of Brewster's Angle to which it reduces if the earth is taken to be loss-free.

7. Geometry of the Attenuating Case

The application of the simple attenuated plane wave to the geometry of the Attenuating Case is very simple. We have seen that when λ is equal to its critical value $2d_{mn}$ the planes of equiphase are parallel to B_mC_n and to the axis of the tube. When λ increases beyond the critical value we use the simple plane attenuated waves, keeping the equiphase planes still parallel to B_mC_n and the tube axis and choosing λ_a such that λ_p remains always equal to $2d_{mn}$. Since the attenuation axis of the simple plane attenuated wave is parallel the axis of the tube λ_a of the wave is also the λ_a along the tube.

Thus we have the simple construction for λ_a shown in Fig. 8, which is, of course, immediately derived from Fig. 7.

The important thing to notice is that when $\lambda \gg 2d_{mn}$, as is usually the case with piston

† Zenneck, *Ann. d. Phys.*, Vol. 23, p. 859, 1907, J. A. Fleming, *Engineering*, June 1909, p. 766.

attenuators, the attenuation length λ_a is nearly equal to $2d_{mn}$.

It has been pointed out that the phase velocity of a simple plane attenuated wave may be very small. As an example consider a square tube of one-inch side being used as a piston attenuator at a frequency of 50 c/s in the 11 mode. For this tube d_{11} is $\sqrt{2}/2$

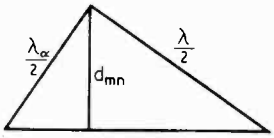

Fig. 8. *Construction for λ_a in the attenuating case.*

inches and therefore $\lambda_p = \sqrt{2}$ inches and the phase velocity $= \lambda_p \times f = 50 \times \sqrt{2}$ inches per second or a trifle over four miles an hour—an ordinary walking pace. To reduce λ_p to this small value of $\sqrt{2}$ inches we introduce a λ_a which is also very nearly equal to $\sqrt{2}$ inch, for in the triangle of Fig. 8, d_{mn} is $\sqrt{2}/2$ inches and $\lambda/2$ about 1,860 miles.

The constructions for λ_t and λ_a are thus simplified and for the important H_{01} case they are shown in Fig. 9.

To obtain λ_t, draw a quadrant of a circle centre A of radius $\lambda/2$ on the upper surface; from C draw a tangent to this circle to cut AA′ at T_{01}; then AT_{01} is $\lambda_t/2$. For λ_a, the construction is equally simple. Draw a circle with centre A and radius AC on the upper surface; extend AC to P so that AP $= \lambda/2$; draw a tangent from P to this circle cutting AA′ in T; than AT $= \lambda_a/2$.

In dealing with the rectangular box resonator it must be pointed out that any one of the three, l, m and n but only one, can be zero. The modifications to the construction given are so obvious that they need not be described.

9. Resolution of Wavelength

The construction considered in Figs. 1 and 5 and the experiment using a bowl of water are more easily appreciated if we introduce the idea of the resolution of wavelength in any direction.

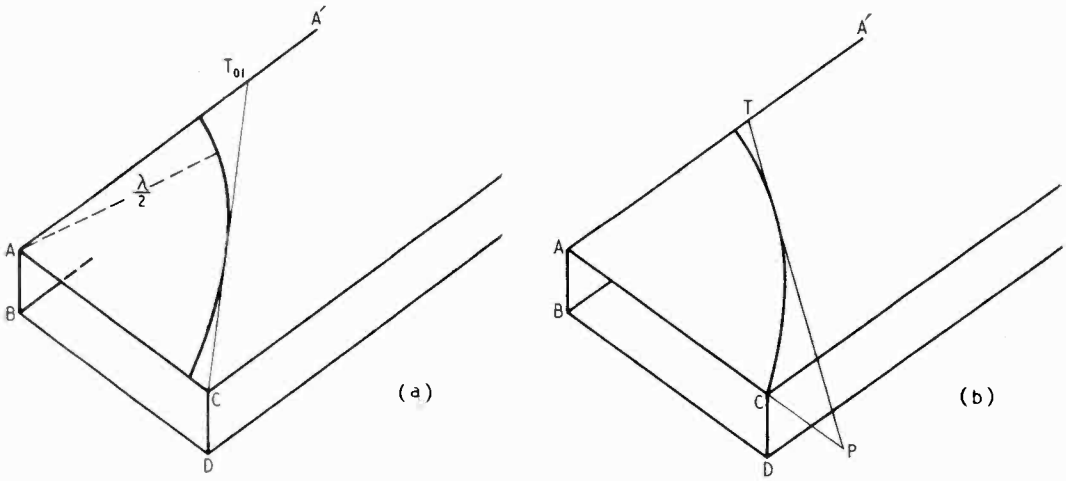

Fig. 9. (*a*) *H_{01}-mode transmitting case; construction for $AT_{01} = \lambda_t/2$;* (*b*) *H_{01}-mode attenuating case: construction for $AT = \lambda_a/2$.*

8. The H_{on} and H_{mo} Modes

Consider the H_{mn} mode in relation to Fig. 1; B_m is a point in AB such that $AB_m = AB/m$; if now m is put equal to zero AB_m becomes infinite. Thus the plane $T_{on}C_nB_o$ is parallel to AB. The corresponding plane for the corner B coincides with this plane and thus the two waves corresponding to the corners A and B coalesce. Similarly the two waves for the corners C and D coalesce and only two plane waves, either standard plane, or simple attenuated, are required to represent the field.

Fig. 10 represents two adjacent equiphase planes. If A is a point in one plane and a perpendicular AN is drawn to the other plane, then AN $= \lambda_p$. Take another point C in the same plane as N and join AC. We may then legitimately call AC the resolved wavelength λ_r in the direction AC, since two observers at A and C who could only measure intensities and who could not move off the line AC would conclude that they were dealing with a wave motion of wavelength λ_r.

There is a very important difference between resolving wavelengths and resolving forces or velocities. A force along AN would have a resolved component AN cos θ along AC but a wavelength λ along AN has a resolute $\lambda_r = \lambda/\cos\theta$ along AC. Referring back to Fig. 1 we see that the construction used to obtain AT_{mn} can be put in the form:—

Orient a standard plane wave so that its resolved half-wavelengths in the directions AB and AC are a/m and b/m respectively, then the resolute along the axis AA′ is $\lambda_t/2$. Similarly for the rectangular box resonator of Fig. 5 we may say that the resonant wavelength for any mode is that $\lambda/2$ which has resolutes a/m, b/n and c/l in three mutually perpendicular directions.

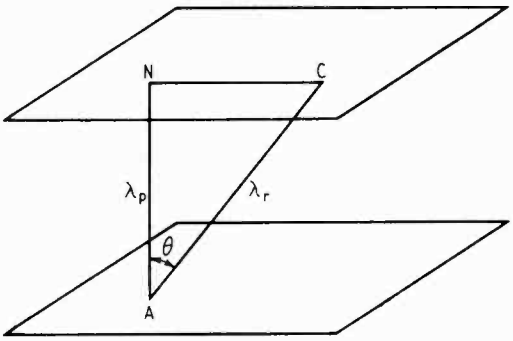

Fig. 10. *Resolution of wavelengths between two equiphase planes.*

10. Plane Waves in a Dissipative Dielectric

So far we have been dealing with vacuum as the dielectric and before we can extend the treatment to the case of a rectangular waveguide filled with a dissipative medium it is first necessary to investigate some of the properties of plane waves in a dissipative dielectric. Since there is an energy loss there must be some kind of attenuation. As will be shown, a little later, the plane wave has a set of parallel planes of equal phase separated by λ_p and a set of parallel planes of equal amplitude separated by an attenuation length λ_a; the two sets of planes can be at any angle.

The wave equation for a dissipative dielectric is—

$$\frac{\delta^2 R}{\delta x^2} + \frac{\delta^2 R}{\delta y^2} + \frac{\delta^2 R}{\delta z^2} - \frac{\epsilon}{c^2}\frac{\delta^2 R}{\delta t^2} - 4\pi\sigma\frac{\delta R}{\delta t} = 0$$

where ϵ is the dielectric constant and σ the conductivity of the medium.

We search for solutions of the form

$$\exp.\{j(\omega t - ax - by - cz) - \alpha x - \beta y - \gamma z\}$$

and proceeding as in Sect. 6 obtain the equation

$$(ja + \alpha)^2 + (jb + \beta)^2 + (jc + \gamma)^2 + \left(\frac{2\pi}{\lambda_1}\right)^2 - j\left(\frac{2\pi}{\lambda_2}\right)^2$$

where λ_1 and λ_2 are two lengths determined by

$$\lambda_1 = \frac{\lambda}{\sqrt{\epsilon}} \text{ and } \lambda_2 = \sqrt{\frac{\lambda}{2\pi c\sigma}},$$

separating real and imaginary parts

$$(a^2 + b^2 + c^2) - (\alpha^2 + \beta^2 + \gamma^2) = \left(\frac{2\pi}{\lambda_1}\right)^2$$

$$2(a\alpha + b\beta + c\gamma) = \left(\frac{2\pi}{\lambda_2}\right)^2$$

As before putting

$$\lambda_p = \frac{2\pi}{\sqrt{a^2 + b^2 + c^2}}$$

and

$$\lambda_a = \frac{2\pi}{\sqrt{\alpha^2 + \beta^2 + \gamma^2}}$$

the first equation gives

$$\frac{1}{\lambda_p^2} - \frac{1}{\lambda_a^2} = \frac{1}{\lambda_1^2} \quad \ldots \quad \ldots \quad (5)$$

a familiar relation which gives the triangle diagram shown in Fig. 11. but does not determine the shape of the triangle.

The cosine of the angle ϕ between two planes $ax + by + cz =$ constant, and $\alpha x + \beta y + \gamma z =$ constant is

$$\cos\phi = \frac{a\alpha + b\beta + c\gamma}{\sqrt{a^2 + b^2 + c^2}\sqrt{\alpha^2 + \beta^2 + \gamma^2}}$$

Fig. 11. *Relation between λ_a, λ_p and λ_1.*

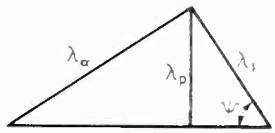

Therefore from the second equation we have

$$\cos\phi = \tfrac{1}{2}\cdot\left(\frac{2\pi}{\lambda_2}\right)^2\cdot\frac{\lambda_p}{2\pi}\cdot\frac{\lambda_a}{2\pi} = \frac{\lambda_p\lambda_a}{2\lambda_2^2} \quad \ldots \quad (6)$$

From the last equation it is seen that when ϕ is nearly $\pi/2$ the product $\lambda_p\lambda_a$ is small, so that the conditions are as shown in Fig. 12 (a); as ϕ diminishes both λ_a and λ_p increase, but there is a limiting value as cos ϕ reaches its maximum value unity; i.e., when the equiphase and equi-attenuation planes are parallel.

For any specified value or ϕ a method to determine the shape of the triangle of Fig. 11 is required. Consider the angle marked ψ in Fig. 11

$$\tan\psi = \frac{\lambda_a}{\lambda_1} \text{ and } \sin\psi = \frac{\lambda_p}{\lambda_1}$$

$$\therefore \tan\psi \sin\psi = \frac{\lambda_a\lambda_p}{\lambda_1^2} = \frac{2\lambda_2^2\cos\phi}{\lambda_1^2}$$

$$\text{whence } \cos^2\psi + \frac{2\lambda_2^2}{\lambda_1^2}\cos\phi\cos\psi - 1 = 0 \quad (7)$$

This quadratic in $\cos\psi$ can be solved algebraically or by the following equivalent graphical construction. Construct a triangle ABC (Fig. 13) with a right angle at A, AC being of length unity and AB of length

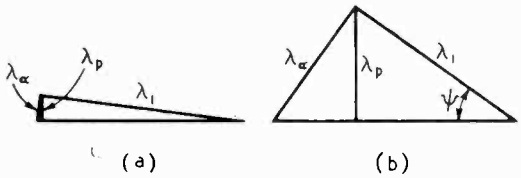

Fig. 12. *Resolution of wavelengths when $\phi \approx \pi/2$ (a) and $\phi = 0$ (b).*

$\lambda_2^2\cos\phi/\lambda_1^2$. Draw a circle centre B, radius BA, to cut BC in E. Construct a semicircle on AC as diameter and then a circle centre C, radius CE, to cut the semicircle in F. Then ACF is the required angle ψ. Since ψ is now known the triangle of Fig. 11 and λ_p and λ_a are fully determined.

11. Rectangular Waveguide with a Dissipative Dielectric

The type of wave discussed in the previous section can now be used to build up the fields of the rectangular waveguide with dissipative dielectric. There are not two entirely distinct cases as with a vacuum; λ_t and λ_a are both always finite and though a division will be made according to whether λ_a is greater or less than λ_t the type of wave is the same in both cases.

As in Sect. 7 the axis of attenuation of the four waves is made parallel to the axis of the tube while λ_p, λ_t, d_{mn} and the propagation axes are related in exactly the same way as λ, λ_t and d_{mn} in the transmitting vacuum case as shown in Fig. 1.

$$\text{Thus } \frac{1}{(\lambda_p/2)^2} = \frac{1}{(\lambda_t/2)^2} + \frac{1}{d^2_{mn}} \quad .. \quad (8)$$

while θ the angle between the direction of propagation and the axis of the tube is given by

$$\cos\theta = \frac{\lambda_p}{\lambda_t}$$

From the previous section we also have

$$\frac{1}{\lambda_p^2} - \frac{1}{\lambda_a^2} = \frac{1}{\lambda_1^2} \quad .. \quad .. \quad .. \quad (9)$$

and ϕ the angle between the propagation axis and the attenuation axis is given by

$$\cos\phi = \frac{\lambda_p\lambda_a}{2\lambda_2^2}$$

From these equations we have to determine λ_a and λ_t. Since we take the axis of attenuation parallel to the axis of the tube

$$\phi = \theta$$

$$\therefore \frac{\lambda_p\lambda_a}{2\lambda_2^2} = \frac{\lambda_p}{\lambda_t}$$

$$\lambda_a\lambda_t = 2\lambda_2^2 = \frac{\lambda}{\pi\sigma c} \quad .. \quad .. \quad .. \quad (10)$$

This simple relation between λ_a and λ_t is dependant only on λ and σ; it is independent of ϵ, of the mode numbers m and n, and of the dimension a and b of the guide. In fact this relation is also true of circular, elliptic and other straight waveguides.

By combining Equs. (8) and (9) we obtain

$$\frac{1}{d_{mn}^2} - \frac{1}{(\lambda_1/2)^2} = \frac{1}{(\lambda_a/2)^2} - \frac{1}{(\lambda_t/2)^2} \quad .. \quad (11)$$

From this we see at once

if $d_{mn} > \lambda_1/2$ then $\lambda_a > \lambda_t$

if $d_{mn} < \lambda_1/2$ then $\lambda_t > \lambda_a$

There is the separating case when $d_{mn} = \lambda_1/2$ and $\lambda_t = \lambda_a$; this is easily disposed of, for since $\lambda_a\lambda_t = 2\lambda_2^2$

$$\lambda_a = \lambda_t = \sqrt{2}\,\lambda_2 = \sqrt{\frac{\lambda}{\pi\sigma c}}$$

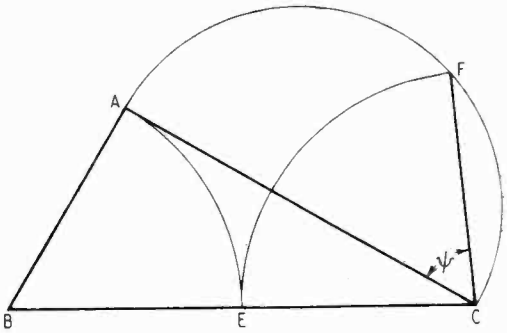

Fig. 13. *Construction to determine the angle ψ.*

It is easily shown that in this case

$$\cos\theta = \frac{\lambda_1}{\sqrt{\lambda_1^2 + 2\lambda_2^2}}$$

The first case, $d_{mn} < \lambda_1/2$, can be dealt with by first determining by a right-angled triangle a subsidiary length D such that

$$\frac{1}{d_{mn}^2} - \frac{1}{(\lambda_1/2)^2} = \frac{-1}{D^2}$$

Having determined D we have from Equ. (11)

$$\frac{1}{(\lambda_a/2)^2} - \frac{1}{(\lambda_t/2)^2} = -\frac{1}{D^2}$$

and therefore the right-angled triangle of

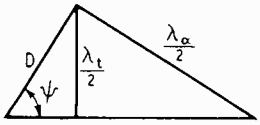

Fig. 14. *Determination of ψ, λ_p and λ_a for $d_{mn} > \lambda_1/2$.*

Fig. 14 in which we have to adjust the angle ψ so that the product

$$\lambda_a \lambda_t = 2\lambda_2^2$$

From the triangle it is seen that

$$\sin\psi = \frac{\lambda_t}{2D} \text{ and } \tan\psi = \frac{\lambda_a}{2D}$$

$$\text{therefore } \sin\psi \tan\psi = \frac{\lambda_a\lambda_t}{4D^2} = \frac{\lambda_2^2}{2D^2}$$

$$\text{whence } \cos^2\psi + \frac{\lambda_2^2}{2D^2}\cos\psi - 1 = 0$$

this equation is solved by the method of Sect. 10 and thus ψ and therefore λ_p and λ_a are determined.

The second case where $d_{mn} < \lambda_1/2$ is treated in a very similar manner. Take an auxiliary length D such that

$$\frac{1}{d_{2mn}} - \frac{1}{(\lambda_1/2)^2} = \frac{1}{D^2}$$

then we have

$$\frac{1}{(\lambda_a/2)^2} - \frac{1}{(\lambda_t/2)^2} = \frac{1}{D^2}$$

and therefore the right-angle triangle construction of Fig. 15 the angle ψ being obtained by exactly the same equation and construction as for the first case.

Fig. 15. *Determination of ψ, λ_p and λ_a for $d_{mn} < \lambda_1/2$.*

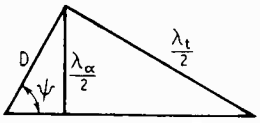

The angle $\theta = \phi$, the angle between the axis of propagation of the four waves and the axis of the tube, is easily obtained, for its cosine is λ_p/λ_t; λ_t is now determined and, from the known values of λ_1 and λ_a, λ_p is obtained from the triangle of Fig. 11.

LINEAR SAW-TOOTH GENERATORS

By A. W. Keen, M.I.R.E., A.M.Brit.I.R.E., Grad.I.E.E.

(Television Dept., Sobell Industries Ltd.)

SUMMARY.—Saw-tooth voltage-wave generators of the hard-valve type usually employ two or more valves in the discharge circuit in addition to a constant-current charging valve. The circuits described in this paper economize in the number of valves required, without sacrifice of wide-range performance, by using the charging valve to assist the action of the discharge circuit during the flyback period.

1. Introduction

THE simple original saw-tooth voltage-wave generator[1] of Fig. 1 (a) has been elaborated[2, 3] in the two ways depicted in Fig. 1 (b) in order to obtain, over a wide frequency range, a substantially linear output having an amplitude comparable with the magnitude of the direct driving voltage V :—

(i) The resistor R (Fig. 1), which causes capacitor C to charge exponentially, according to the law†

$$v = V\left(1 - e^{\frac{-t}{CR}}\right)$$

has been replaced by " electronic " constant-current devices ; e.g., a pentode (or tetrode)[4] operating on the (nearly) " flat top " portion above the " knee " of its anode (V_A–I_A) characteristic. In later developments[5,6] good use has been made of negative feedback arrangements, as in the Blumlein-Miller integrator[7].

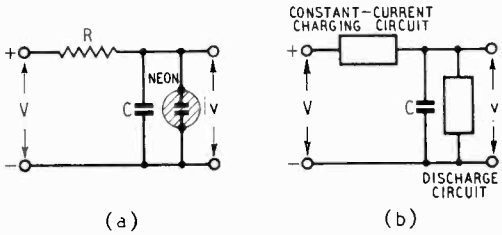

Fig. 1. *(a) The original saw-tooth voltage-wave generator ; (b) generalized form of the generator circuit typified by (a).*

† Assuming $v = q = 0$ at $t = 0$.

MS accepted by the Editor, March 1947.

(ii) The gas-filled discharge tube (neon) has been superseded (after the gas-filled triode) by circuits, usually of the "trigger" type[8], involving one or more hard valves, in order to obtain improved stability and synchronization and to extend the usable frequency range.

Thus a practical generator capable of operating satisfactorily over a wide range of conditions may require several valves. For instance, the very successful time-base circuit developed by Puckle[9], which is still widely used in general-purpose oscilloscopes, requires not less than three valves.

When it is desired to minimize the number of valves it is usual to dispense with the charging valve[10], but the resultant loss of linearity may be intolerable. Again, the number of valves in the discharge circuit may be reduced to one by employing regenerative coupling through a phase-reversing transformer between the input and output circuits of the hard discharge valve[11], but such arrangements fail at high sweep frequencies. Application of the transitron principle also allows the use of a single hard valve in the discharge circuit[12, 13, 14, 15]. Transitron trigger action may also be employed in the charging valve to achieve flyback[16]. It may be fairly stated, however, that all these attempts at simplification of the hard-valve time base have, as yet, failed to produce a time-base generator suitable for wide-range oscilloscopes and having fewer valves than those circuits generally used for this purpose.

The object of the present paper is to describe briefly a type of circuit which satisfies the latter requirement while using only two valves. The distinguishing feature of the circuit is the use of the charging valve to assist the discharge valve during the flyback period; there are other special features and applications which will be mentioned later.

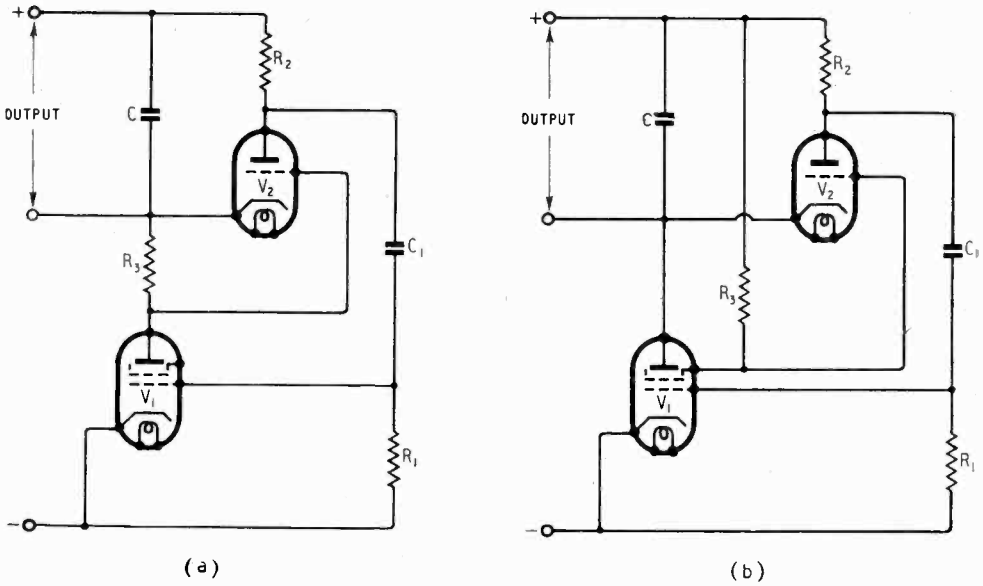

Fig. 2. *Basic circuit configurations employing the principle of using the constant-current charging valve to assist the action of the discharge circuit; (a) anode-coupled case: (b) screen-coupled case.*

2. Basic Circuits

Formal application of the principle just stated to the basic generator arrangement shown in Fig. 1 (b) yields the two circuit configurations of Fig. 2 which differ in the method of "holding off" the discharge valve during the capacitor-charging period. In case (a) the anode current of the charging valve V_1 is passed through a resistor R_3. This is included also in the grid-cathode path of the discharge valve V_2 and the current develops sufficient bias to cut-off the latter. In case (b) the screen current of the charging valve V_1 is used to develop the cut-off bias.

The circuit action in both cases is broadly as follows:—

Charging Period.

Commencing with capacitors uncharged and cathodes emitting, the application of

H.T. voltage to the circuit terminals in the direction indicated causes C to charge through V_1 (nearly linearly, because V_1 is operating above the "knee" of its anode characteristic). The discharge valve is prevented by the voltage developed across R_3 from passing current until its cathode potential has fallen sufficiently to make its anode-cathode p.d. large enough to overcome its negative grid-to-cathode p.d. In case (a) the latter remains substantially constant; in case (b) it falls as the anode-cathode p.d. rises.

Discharge Period.

When V_2 starts to conduct, the resultant negative-going potential change at its anode is communicated by C_1R_1 to the control grid of V_1; as a result both the anode and screen currents of this valve fall and reduce the p.d. across R_3, thus driving the grid of V_2 less negative with respect to its cathode and allowing the discharge current to increase. This action is cumulative (until V_1 reaches cut-off), so that C is discharged very rapidly. Actually the grid of V_1 is driven beyond cut-off for a period which depends on the grid circuit time-constant. When C_1 has discharged sufficiently to allow V_1 to conduct again, V_2 is cut off and the cycle repeats.

It is interesting to compare these basic circuits with similar types already described in the literature. The anode-coupled form (a) may be derived by arranging the circuit of Fruhauf[17] for central-battery operation and substituting a constant-current pentode for one triode. The screen-coupled version (b) bears comparison with the three-valve version of the Puckle (Ref. 3, p. 31) circuit if the charging valve is regarded as performing the functions of both pentodes of the latter circuit.

3. Theoretical Discussion

Before proceeding to elaborate these two basic circuits, it is desirable to examine their action in detail from the following points of view :—

(i) The degree of linearity of the capacitor charge, and

(ii) The rapidity of the capacitor discharge.

Linearity of Charge.

The linearity is governed largely by the characteristics of the charging valve. In considering the extent to which these characteristics are influenced by operating conditions in the associated circuits, the following factors are involved :—

(a) The capacitor C must not be allowed to charge sufficiently to bring the anode potential close to the "knee" of the anode characteristic. It will be noted that in the case of Fig. 2 (b) serious "bottoming" cannot occur since the grid of V_2 is at the screen potential of V_1. Consequently V_2 begins to conduct before the anode potential of V_1 reaches that of its screen.

(b) Negative feedback may be applied in various ways to improve the linearity of the charge.

(c) After each flyback the anode current must rise quickly to its normal value without overswing.

(d) Low reactance values of stray circuit parameters cause waveform deterioration at extreme operating frequencies.

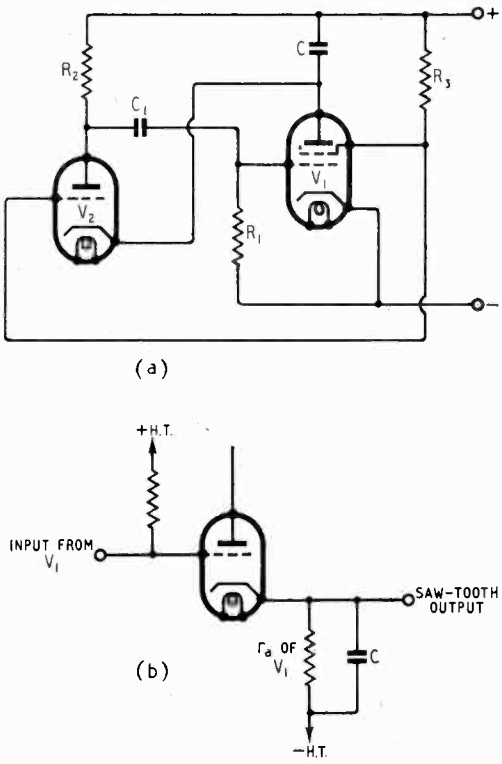

Fig. 3. *The basic screen-coupled circuit of Fig. 2 (b) redrawn to bring out (a) the amplifier, and (b) the cathode-follower aspects of the circuit action.*

Rapidity of Discharge.

The rate of the discharge of C depends largely on the effective resistance of the discharge valve together with its anode load and no difficulty is experienced at the lower operating frequencies in obtaining a sufficiently rapid flyback. At high frequencies the flyback time is limited by the retarding effect of stray capacitances on the current-controlling electrodes. The operation of the circuit during the flyback period at high operating frequencies is best understood by considering the h.f. response of the entire discharge circuit loop, regarded as an amplifier. The basic circuit for the screen-coupled case has been redrawn from this viewpoint in Fig. 3 (a).

On this basis it is evidently advantageous to adopt the methods of h.f. compensation employed in v.f. amplifiers in order to minimize flyback time at the higher end of the frequency range of the generator.

In addition to the regenerative feedback occurring over the principal loop comprising the feedback circuit, it will be observed that a cathode-follower action occurs with consequent effect upon the circuit action and on the effective parameters of the discharge valve. This point is clarified in Fig. 3 (b).

4. Experimental Results

Experimental investigation has confirmed that the two basic configurations shown in Fig. 2 function readily as saw-tooth generators; the screen-coupled case (b) is generally the more satisfactory and a typical development of this form is given in Fig. 4.

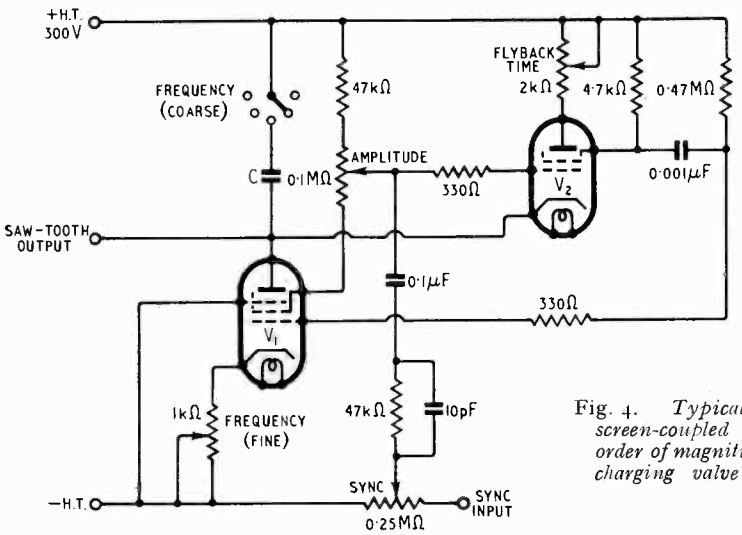

Fig. 4. *Typical practical development of the screen-coupled case of Fig. 2 (b) showing the order of magnitude of the component values; V_1 charging valve Mazda SP61; V_2 discharge valve 807.*

A variety of valves has been used successfully in both circuits; in general, types developed for v.f. amplification (i.e., having a high slope and small interelectrode capacitances) are the most suitable, an excellent combination being the SP61 for V_1 and 807 for V_2, particularly at high sweep frequencies.

The following steps have been found effective in reducing flyback time:—

(a) Substitution of a high-slope, high-current tetrode (or pentode) for the conventional low-impedance triode in the discharge circuit (V_2).

(b) Connection of the load impedance of V_2 in its screen circuit leaving the external anode-cathode circuit impedance free.

(c) Return of the grid resistor of V_1 to +H.T. instead of − H.T.

(d) Use of a short time-constant coupling (C_1R_1) between the grids of V_1 and V_2. This step reduces the output amplitude by allowing V_1 to re-conduct before the discharge of C is complete.

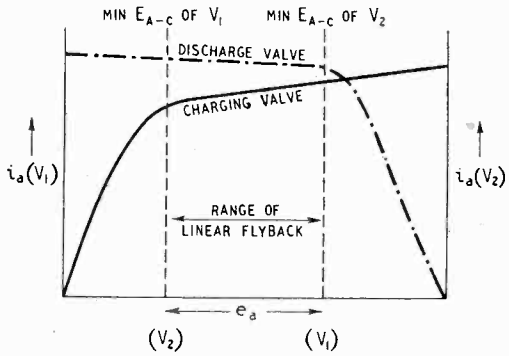

Fig. 5. *Use of a constant-current discharge valve to linearize the flyback.*

An important and distinctive feature of the circuits under consideration arises from the action of the coupling (C_1R_1) between the anode (or screen) of V_2 and the grid of V_1. The start of current flow in the discharge-

valve load produces a negative-going voltage step which may be differentiated by making the feedback time constant sufficiently small, thus producing a short negative "peaky" pulse on the grid of V_1. If this pulse is sufficiently brief V_1 may become conductive again before C has completely discharged. This fact not only allows a very short flyback time to be achieved (at the expense of amplitude) but, if a tetrode (or pentode) is employed in the discharge position, its operating point may be restricted to the flat-top of its anode characteristic, as shown in Fig. 5, thereby linearizing the flyback.

The parameters of the voltage wave generated may be varied in the customary manner, viz.—

(i) Amplitude—by alteration of the grid potential of V_2.

(ii) Frequency—by switching charging capacitance C (coarse) and by varying the cathode, grid, or screen potentials of V_1 (fine).

(iii) Flyback Time—by a small variable resistor in the anode circuit of V_2.

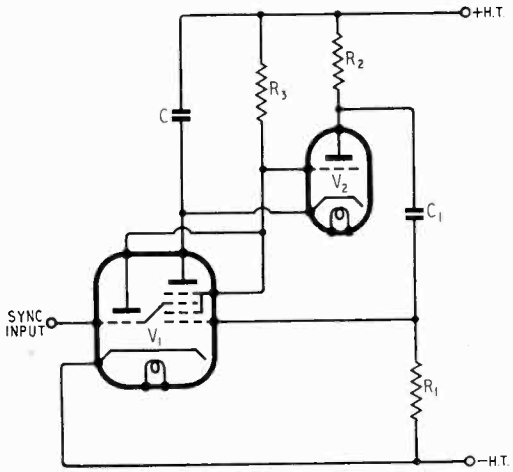

Fig. 6. *A triode-hexode charging circuit incorporating sync amplification.*

Care must be exercised in applying the synchronizing voltage otherwise the charging current flowing through V_1 may be seriously disturbed. In the case of pulse operation the triggering wave may be applied to the suppressor grid of V_1, but in most oscilloscopes the grid of V_2 must be employed. An interesting development using a triode-hexode valve of the frequency-changer type for V_1 is shown in Fig. 6; this form not only provides satisfactory synchronization under all conditions, but is readily adapted to single stroke working.

5. Conclusion

The application of a new principle in linear saw-tooth wave-generator design (viz., the inclusion of the constant-current charging valve in the discharge-circuit loop) yields a new type of circuit capable of development into efficient practical wave generators characterized by satisfactory performance in regard to linearity and flyback time over a wide frequency range. The flyback may be linearized at the expense of amplitude reduction. Another special feature of these circuits is their adaptability to ratchet-operation.

6. Acknowledgment

The writer wishes to acknowledge his indebtedness to Sobell Industries Ltd. for permission to publish this article and to O. S. Puckle for careful criticism of the MS.

REFERENCES

[1] (*a*) S. O. Pearson and H. St. G. Anson. "The Neon Tube as a Means of Producing Intermittent Currents." *Proc. Phys. Soc.* London, 1922, Vol. 24, Pt. V, p. 204.
(*b*) H. St. G. Anson. British Patent Specification, No. 214,751.

[2] M. Von Ardenne. (Translation by G. S. McGregor & R. C. Walker.) "Cathode Ray Tubes," Ch. II. 4, para. 2 (*c*), pp. 265–276. "Sawtooth Discharge Circuits Using Hard Valves." Pitman, 1939.

[3] O. S. Puckle. "Time Bases," Chapters III (pp. 11–35) and VII (pp. 81–96) and Appendices II and III. Chapman and Hall, 1943.

[4] O. S. Puckle—reference 3, p. 14.

[5] F. R. Norton, British Patent Specification No. 467,958.

[6] W. R. Groves, *Wireless World* (letter), September 22, 1938, p. 278.

[7] F. C. Williams, "Introduction to Circuit Techniques for Radiolocation." *J. Instn elect. Engrs*, Vol. 93, Pt. IIIA, No. 1, 1946, pp. 303–4.

[8] O. S. Puckle, reference 3, Ch. IV. "Trigger Circuits," pp. 36–62.

[9] O. S. Puckle, reference 3, pp. 30–35, or original paper, "A Time Base Employing Hard Valves." *Journal of the Television Society*, Series II, Vol. 2, Pt. V, June 1936, pp. 147–155. Also: British Pat. Spec. No. 419,298.

[10] J. L. Potter, "Sweep Circuit," *Proc. Inst. Radio Engrs*, June 1938, Vol. 26, No. 6, pp. 713–9.

[11] W. T. Cocking, "Television Receiving Equipment," pp. 89–97 Iliffe, 1940.

[12] E. L. C. White, British Patent Specification No. 455,497.

[13] H. M. Lewis, British Patent Specification No. 530,227.

[14] B. C. Fleming-Williams, "A Single-Valve Time-Base Circuit," *Wireless Engineer*, 1940, Vol. 17, p. 161.

[15] H. J. Reich, "Trigger Circuits," *Electronics*, August 1939, p. 14.

[16] W. T. Cocking, "Linear Saw-tooth Oscillator," *Wireless World*, June 1946, pp. 176–8.

[17] W. Fruhauf, *Arch. f. Elekt.*, Vol. 21 (1927), p. 471.

TRANSMISSION-LINE BRIDGE

Applications to Directive Arrays

By C. H. Westcott, Ph.D.

(Physics Dept., Birmingham University, formerly of Telecommunications Research Establishment)

1. Introduction

IN the course of certain development work on 200-Mc/s radar ground stations for the R.A.F. during the war, a transmission-line bridge with interesting general properties was devised. The present paper gives a detailed treatment of the behaviour of this system with illustrations of its use. Taylor and Westcott[1] have already published a description of the aerials developed for the radar stations with which this work was connected and have considered this feeder bridge in general terms, so that it is unnecessary here to describe the aerial systems in any detail. It should, however, be made clear that the aerials were directive broadside arrays generally consisting of four or five similar "bays" side by side, and that twin open-wire feeder of 330-Ω characteristic impedance was used, consisting of 200 lb per mile copper wires spaced $\frac{7}{8}$ in.

2. The Feeder Bridge

Consider the bridge shown in Fig. 1, consisting of four $\lambda/4$ sections of line AB, BC, CD, and DA connected in a re-entrant loop, one of the sections (DA) containing a transposition of the two wires of the feeder. Suppose feeders, correctly terminated by $Z_0 = 330$-Ω loads, be connected to the bridge at the points B and D, and imagine an r.f. generator connected at A. If we place a short-circuit at the point C, each of the arms BC and CD of the bridge become short-circuited quarter-wave stubs, and as such present infinite impedance at the points B and D respectively. From another point of view, we may say that complete standing waves occur on these arms, with a voltage node at C and current nodes at B and D, so that no current is drawn at the latter points. The power from the generator at A will, therefore, divide equally (by symmetry) into the two loads attached to B and D, but owing to the transposition in DA, the points B and D (as well as the two loads, if the feeders to them are of equal length) will be fed in antiphase. Moreover, the generator will be working into an impedance of $Z_0/2$ (= 165 Ω), due to two correctly matched feeders connected in parallel at A.

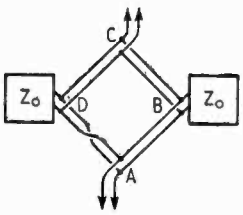

Fig. 1. *The feeder bridge; all feeders have* $Z_0 = 330\ \Omega$; $AB = BC = CD = DA = \lambda/4$.

Now if we consider the arms BC and DC to be separately short-circuited, the current in either shorting bar will be V_B/Z_0 or V_D/Z_0 amperes, where V_B and V_D are the voltages across the lines at B and D respectively. In fact, there is only one shorting-bar carrying a current $(V_B + V_D)/Z_0$ amperes, with of course no volts across it. But we have just shown that B and D are fed equally and in antiphase, consequently $V_B + V_D$ is zero. The shorting-bar therefore carries no current, and has no volts across it; consequently it may be removed and any other load whatever connected at the point C of the bridge without affecting the operation of the system due to the generator at A. The only requirement for this to be true is one of symmetry; i.e., the impedances of the loads attached at B and D must be equal. It is not necessary for them to be correct terminations for the feeders employed.

It may be shown similarly that if a generator be attached at C, no voltage or current appears at A, the power being again divided equally between the loads attached at B and D but this time the two loads are connected in phase instead of antiphase. It is thus possible to have two generators connected simultaneously, one at A and one at C, and neither of them will tend to feed power into the other. Moreover, each generator appears matched into a $Z_0/2$ (= 165 Ω) load irrespective of whether the other is connected or working or not.

The case of simultaneous working of the two generators on the same frequency is of

MS accepted by the Editor, March 1947

some interest, since the distribution of power between the loads depends on the phase-relation of the sources. Thus if the two generators are in phase their currents in the load attached at B will add up, whereas at D they will cancel, so that all the power from both generators will pass into the load B and none into the load D. Similarly if the generators are in anti-phase all the power will go into load D and none into B, while if they are in quadrature the power will divide equally between the loads as it would if only one generator were operating. But in all cases each generator will appear to be working into a $Z_0/2$-Ω load at A or C respectively. These properties are most readily seen by using the principle of superposition, the two fundamental modes being those in which only one of the two generators is operating. The general case is then obtained by adding at all points the voltages (or the currents) which result from each of these modes alone, taking any proportion of the two modes and any phase difference between them.*

3. Application to Directive Transmitting Arrays

A particular application of this feeder bridge occurs in connection with directive broadside arrays. Fig. 2 shows, for example,

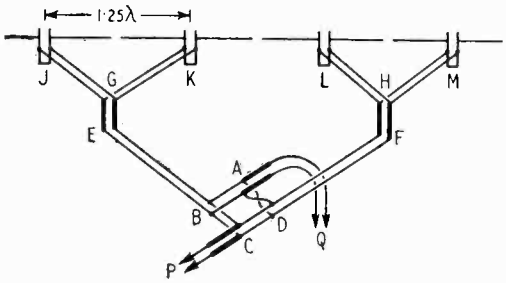

Fig. 2. *Feeder bridge used with 4-bay array.*

how the bridge can be used with a 4-bay array similar to that described by Taylor and Westcott.[1] In this case four similar "bays" J, K, L, and M are placed 1.25λ apart in front of an aperiodic wire-netting reflector, and the feed-point to each bay has a 330-Ω impedance. The pairs J, K and L, M are first paralleled as shown at G and H, the feeders GJ, GK, HL and HM being all equal in length, and quarter-wave transformers EG and FH of $Z_0 = 330/\sqrt{2} = 234\,\Omega$ used to transform the resulting 165-Ω impedance back to 330 Ω. Equal feeders BE and DF are then used to connect the feeder bridge to E and F as loads, and further 234-Ω λ/4 transformers used at A and C so that the main feeders P and Q are correctly terminated.

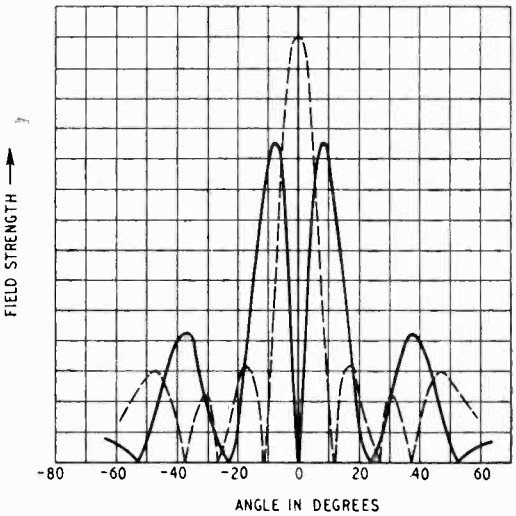

Fig. 3. *Horizontal radiation diagram for 4-bay array;* – – – – – – *4 bays at* 1.25 λ (1, 1, 1, 1); ——— *4 bays at* 1.25 λ (−1, −1, 1, 1).

It should be clear from the preceding paragraph that if a transmitter is connected to feeder P, the power will divide equally between the feeders BE and DF, and E and F will be energized in phase. By symmetry, the power will again divide equally at G and H, with the result that all four bays will be energized equally and in phase. However, if the transmitter is connected to feeder Q, bays J and K will be in antiphase with L and M, and this will result in a different radiation diagram for the array as a whole, as shown in Fig. 3. For example, the radiation normal to the array will be a maximum if feeder P is used, but zero if Q is used, as might be seen by symmetry. In either case it is also clear that the feeders P and Q are correctly matched to the array, and no standing waves should be produced. Even if, in practice, the bays should be of slightly incorrect impedance so that standing waves appear (these generally did not exceed

* For the case of the two generators in phase the matching may also be examined by realizing that the load at D may be removed (since no current flows in it) as well as the arms AD, CD of the bridge, which merely behave as short-circuited λ/4 stubs. We then have a case analogous to that considered in Section 4, by which methods it may be shown that each generator provides half of the load current and sees an impedance of $2Z_0$ (=660 Ω in our case) at the junction point B. The λ/4 sections AB and CB then transform this to 165 Ω at A and C respectively, in agreement with our earlier result.

3 : 2) the symmetry of the whole system will assist in ensuring that the loads seen at B and D are equal so that the bridge works as described.

4. Matching of Receiving Arrays

It is general when designing directive arrays to consider the matching for the transmitting case, even if the aerial is to be used for reception, and to assume that this match will be correct for the reciprocal condition. For example, if we consider the two bays, J, K (Fig. 2) and treat E as attached to a 330-Ω load, which will be transformed to 165 Ω by GE, we see that the system is equivalent to Fig. 4. The matching condition now becomes the condition for maximum power-transfer, which is usually that the load shall equal the generator impedance, and that half of the power generated reaches the load. In our case we have

$$E_1 - Zi_1 = E_2 - Zi_2 = (i_1 + i_2)R$$

whence by addition

$$E_1 + E_2 = (Z + 2R)(i_1 + i_2)$$

and the power in the load becomes

$$R\,(i_1 + i_2)^2 = \frac{R(E_1 + E_2)^2}{(Z + 2R)^2}$$

The optimum R is easily seen to be $\frac{1}{2}Z$, as would be expected, and is independent of the phase-difference of E_1 and E_2, except of course that if $E_1 = -E_2$ no power reaches the load and the result is indeterminate. However, unless $E_1 = E_2$ it is easily seen that less than half the power generated $(E_{1i1} + E_{2i2})$ reaches the load, so that the normal matching condition does not apply—in the extreme case of antiphase generators already mentioned no power reaches the load at all. Reverting to the system EGJK of Fig. 2, we see that this means that although the optimum load has been chosen, there is a partial reflection of energy at G for all cases except that in which the voltages induced in J and K are in phase.

If we consider what this means in the behaviour of the array, we see that if the incoming wave is incident along the normal to the array the voltages induced in the two bays will be equal and in phase, and all the power will pass down the feeder system. However, this is not so in other cases, and part of the power will be reflected at G and re-radiated. If the angle of incidence is such that the two bays are energized at 180° out of phase (i.e., incident ray at 23.6° to the array-normal in our case) the whole of the energy is reflected at G and re-radiated. It is because of this property of reflection at a junction that the pair of bays in parallel can form a more directive aerial than either separately. This form of reflection must be carefully distinguished from the reflection of energy caused by mis-matching the feeder, for we have already chosen the optimum load and matched the system as well as we can. Both forms of reflection cause loss of signal and the re-radiation of energy, but the form of reflection we have considered is inherent in the action of a multi-element directive array.

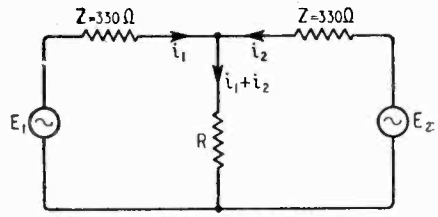

Fig. 4. *Equivalent circuit, E_1, E_2, i_1 and i_2 are all complex quantities on the usual convention (i.e., multiply by $e^{j\omega t}$ and take the real part).*

5. Feeder Bridge Applied to a Receiving Array

If we now consider the complete array of Fig. 2 we shall be able to appreciate the action of the feeder bridge when the feeders P and Q are each matched to receivers. If the incident radiation arrives along the line of shoot, so that all four bays are energized in phase, all the power will pass down the feeders EB and FD, the points B and D being in phase. Consequently all the power will pass by way of C to feeder P, just as if BA, DA, and feeder Q did not exist, and Q will receive no power. However, if the radiation is incident at 11.55° to the array-normal, J and K will be energized in quadrature. Some of the energy will be lost by reflection at G and H, but the remainder will arrive at B and D in antiphase. Had the system leading to feeder Q been removed this would all have been reflected at C and re-radiated; in fact feeder P receives no power but all that comes down EB and FD passes into feeder Q. We can thus obtain on the two receivers two different polar diagrams, viz., those of Fig. 3, quite independently of one another. Neither receiver absorbs any power that might have reached the other

one, absorbing only power that would have been re-radiated if the other receiver only had been connected using normal methods. The matching of either receiver to its feeder is quite normal and quite unaffected by the presence of the other receiver.

6. A Radar Application

The feeder bridge described above has found several applications. A principal one is for lobe-narrowing. On the plan-position indicator (p.p.i.) display[4] an echo appears as an arc whose length corresponds to the beam-width of the aerial, and the display is much improved if this arc is shortened. To obtain a narrower beam directly would often involve a prohibitive increase in aerial aperture, but by using the feeder bridge an auxiliary receiver can be made to respond only to off-bearing targets, and if its output is used to cancel (at video-frequency) the output of the main receiver, the response can be made to appear only over a reduced arc. A disadvantage is that the noise level is increased by using two receivers, but in many cases this can be tolerated.

In the actual applications a five-bay array was used, as shown in Fig. 5. The centre bay is fed in phase and in parallel with all the other bays from feeder P as shown, while feeder Q corresponds to bays J and K fed in anti-phase with M and N, the centre bay L not being energized by this feeder. The resulting radiation diagrams are as shown in Fig. 6; it will be seen that these are similar to those of Fig. 3 but the side-lobes are much reduced, which was the main reason why

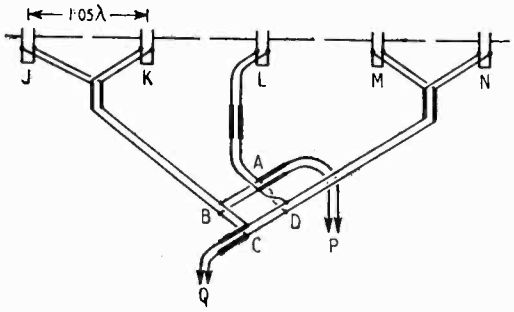

Fig. 5. *Feeder bridge used with 5-bay array.*

a five-bay system was adopted. Feeder P was connected to a common-aerial device[2], so that it could be fed from the transmitter as well as feeding the main receiver, while Q was connected to the auxiliary or "narrowing" receiver. According to theory none of the transmitter power reaches feeder Q, so that common-aerial protection for this receiver should not be required; in practice it was usual to connect a spark-gap across the feeder to deal with accidental unbalance of the bridge, but this gap did not normally "strike," showing that very little trans-

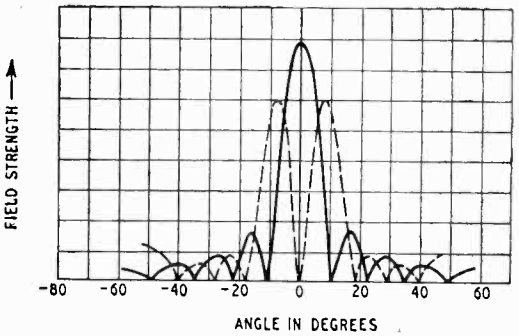

Fig. 6. *Horizontal radiation diagram for 5-bay array;* ———— *5 bays at* 1.05 λ (1, 1, 1, 1, 1); - - - - - - *5 bays at* 1.05 λ (−1, −1, 0, 1, 1).

mitter power reached this feeder. In fact, the behaviour of the system was very closely as expected; no particular difficulty was experienced in ensuring that substantially equal loads were attached at B and D to "balance" the bridge, and the system did not introduce abnormal standing waves at any point on the feeder. The system was monitored for standing waves with the device described by Lees, Kay, and Westcott[3] and was not found to be appreciably more critical than the arrays without the feeder bridge in matters of setting up and maintenance. Normal care was all that was needed to ensure sufficient symmetry between the two sides of the array.

The effective receiver sensitivity diagrams obtained for different relative gains of the main and auxiliary receivers are shown in Fig. 7, where the increase in noise-level for each curve is also indicated. The negative portions of the curves correspond to "noise-suppression;" on the display used the positive peaks of the noise are usually set so as just to begin to produce brightness, and when a signal is received at greater strength on the auxiliary receiver, these peaks are suppressed. However, these negative lobes are much reduced because they tend to occur at angles at which the transmitter radiation diagram is near a zero, so that in the overall diagram (Fig. 8) only the first one is of any appreciable size. In order to ensure that this effect occurs

the use of a common transmitting and receiving aerial system is advisable, or alternatively exactly similar aerials with accurate following in azimuth.

In practice the system behaved very much as expected. Some care was necessary to ensure that the pass-bands of the two receivers were similar, so that the contour of the pulses produced was similar, but the condition was not unduly difficult to meet. It was also found desirable to include a volume control in the video-mixing unit for "narrowing" control, rather than use the normal screen-voltage control in either amplifier, the two amplifiers being set to much the same gain initially. The "holes in the noise" were noticeable but not troublesome—they represent regions within which two signals from exactly the same range would not be truly resolved. It should be realized that although this method improves the presentation, it does not really improve the resolution of two targets differing only in azimuth and less than a beam-width apart, since such signals will "beat" together so long as both are within the beam. The only way to improve the true resolution is to use a wider aerial or a shorter wavelength. Nevertheless, for targets some 10–15° apart the system gives an appreciable improvement, since it gives two dots which are quite distinct (each being outside the beam of the other) whereas on the original presentation the two long arcs would merge and it would be difficult to estimate the centre of either. For this reason the system did, in practice, appear to give some increase of resolution for two signals of approximately equal amplitude, though if one signal were say ten times larger than the other the smaller signal would disappear on this system at about the same angular displacement at which resolution would cease in any case. Such effects are not of great operational importance however since they only occur for two targets at precisely the same range.

Another advantage of the system was the suppression of interference from "unlocked" pulses due, for example, to transmission from neighbouring stations of the radar chain. On the normal displays these all produced bright points on the screen, being strong enough to be received at all azimuths of the aerial. On this system, however, at most angles the response would be negative (Fig. 7 applies to this case, not Fig 8.) so nothing would appear. A further improvement resulted if the overload level of the auxiliary receiver was set higher than that of the main receiver, since then nearly all very strong signals came out negative. At a few azimuths bright signals might appear, but the improvement was very noticeable in practice.

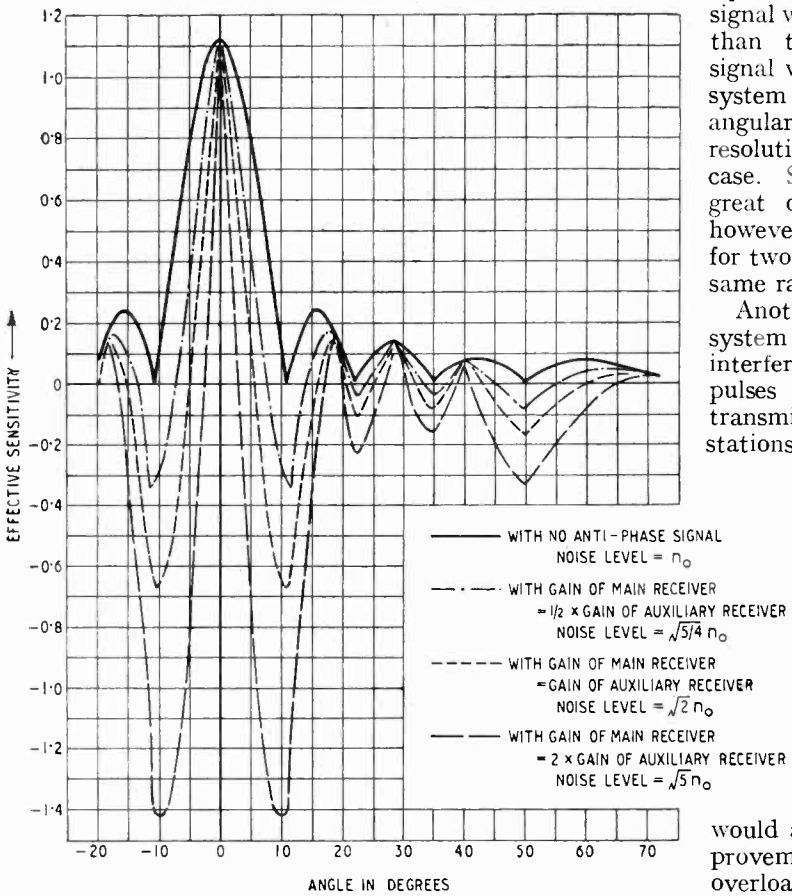

Fig. 7. *Effective receiver azimuthal sensitivity diagram.*

7. Other Applications

The system has been adopted fairly considerably for identification or i.f.f. systems used in conjunction with a radar using a shorter wavelength and therefore having an inherently narrower beam than the i.f.f. system. The aerials are of rather different form in this case, but it should be noted that it is the curve corresponding to Fig. 7 (not Fig. 8) which applies in these systems. The suppression of "clutter" from unlocked pulses is also of importance in this application, and the large negative side-lobes do not appreciably affect the resolution of two signals from the same range, since both signals will be intermittent and each is readily seen in the intervals of the other transmission.

Another application was to the production of "split beams"[1] with common aerial working. Here the object of the feeder bridge is to obtain a feeder system requiring only one common-aerial device, as explained above. By recombining the outputs of feeders P and Q in quadrature we then obtain a single lobe displaced sideways from the original position; and by reversing the phase of one of the feeders with respect to the other we obtain the lobe displaced in the opposite direction. The recombination is in this case done by rejoining the receiver feeders, and a suitable point to arrange the phase-reversal is at the balance-to-balance transformer.

In conclusion, it should be noted that the feeder bridge described may be used quite satisfactorily over a fairly wide band of frequencies, since its action depends on symmetry only. At frequencies at which the arms are not exactly $\lambda/4$ long the only effect will be that the two arms leading to the other feed-point behave like separately short-circuited stubs and throw some reactance across the load, but if two loads attached are similar, the bridge will still behave as described above. The bridge may also be used with concentric cables, but in this case it will be necessary to make the arm DA $3\lambda/4$ long instead of introducing a transposition. As long as the cables used are not unduly lossy, the action will be just as described for the twin-feeder case, but the wide-band property will be somewhat impaired.

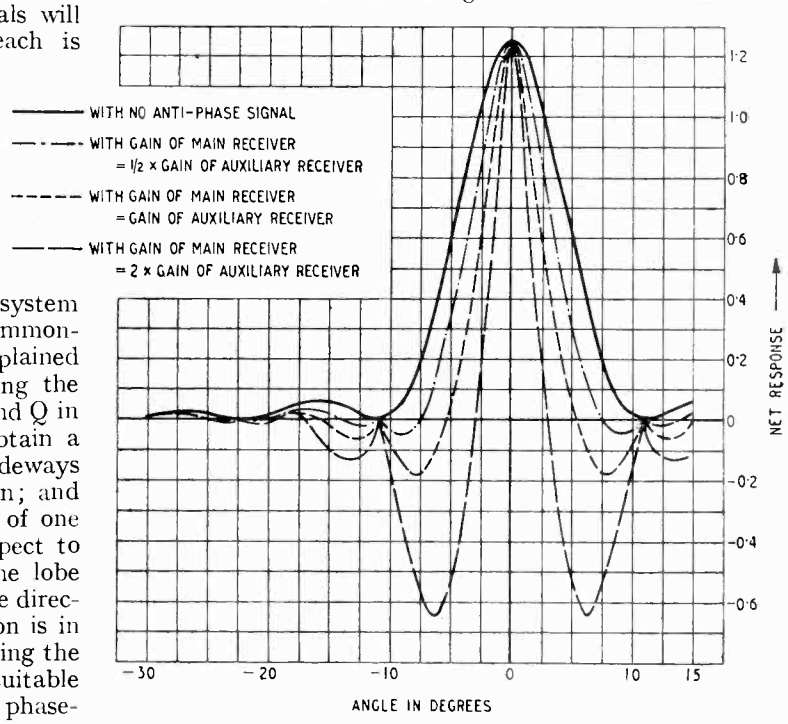

Fig. 8. *Overall azimuthal diagram (transmitter radiation × receiver sensitivity).*

8. Acknowledgments

The work was done as part of the war-time programme at the Telecommunications Research Establishment, and the author is indebted to the Ministry of Supply for permission to publish. He also wishes to thank his colleagues who have contributed in discussion and in the execution of the experiments. The use of the device described in this paper is the subject of British Patent No. 23499/44.

REFERENCES

[1] D. Taylor and C. H. Westcott. "Divided Broadside Arrays with Application to 200 Mc/s. Ground Radiolocation System." *J. Instn elect. Engrs*, Vol. 93, Part IIIA, p. 588.

[2] C. J. Banwell. *J. Instn elect. Engrs*, 1946, Vol. 93, Part IIIA, p. 545.

[3] R. J. Lees, F. Kay, and C. H. Westcott. "Transmission Line Impedance Measurement." To be published in *Wireless Engineer*.

[4] G. Bradfield and others, *J. Instn elect. Engrs*, 1946, Vol. 93, Part IIIA, p. 128.

SCREENING AT V.H.F.

Efficacy of Metallic Surfaces

By B. Roston, B.Sc.(Eng.), A.M.I.E.E.

(The British Electrical and Allied Industries Research Association)

SUMMARY.—The paper aims at examining the v.h.f. screening properties of the various metallic surfaces which are economic and which may be readily adapted to production. An analysis of the problem of shielding shows that in the case of a receiver, where only the radiation field requires to be screened, a conducting sheet makes an efficient shield. The shielding of a source or of a receiver *near* a source is relatively more difficult, since the induction field may predominate and only a thin surface layer of a shield is effective in neutralizing this component of the field.

An experimental method has been developed by which the efficacy of various forms of metallic shield may be assessed. Tests upon electro-deposited steel specimens and sprayed-metal specimens have given results which confirm the theoretical deductions and determine the order of their screening efficacy.

1. Introduction

METALLIC shields are used extensively at very high frequencies for the purposes of screening sources of interference and interference-suppression apparatus, as well as for more general purposes in receivers and their associated equipment. It has been shown previously[1] that in order to secure adequate suppression, it is essential to shield the source in the case of interference generated by electro-medical apparatus and by ignition systems and other electrical equipment on vehicles. The screening of electro-medical apparatus requires the construction of a shield sufficiently large to enclose the patient and operator as well as the apparatus itself, and it is often desirable to screen the whole room in which the equipment is situated. The cost of such a shield may be reduced to an economic value by the use of wire netting, sprayed metal or paper-backed metallic foil.

The screening of ignition systems on vehicles and aeroplanes should be complete to be effective. This requires the use of screened sparking-plugs, distributor and coil or magneto. These components must be connected by screened ignition leads passing through metallic glands. Such a system is both spacious and expensive if robust metallic shields are used throughout, and it is therefore common practice to shield only the ignition leads with metallic braiding, but there exists a demand for the introduction of an inexpensive yet effective form of shield for the remaining components of the circuit. Shields in the form of metal sprayed upon a plastic base and of metal electro-deposited upon a steel base would appear to meet the current production requirements if they can be shown to possess adequate screening properties. Other electrical equipment requiring screening includes the voltage regulator and the wiring system associated with the various motors and generators, these machines being themselves adequately screened by their casings. A lower degree of screening will suffice for this equipment than for the ignition system because the interference voltage generated is considerably lower. It is usual as before to screen the wiring system by means of metallic braiding.

The present investigation aims at examining the v.h.f. screening properties of the various metallic surfaces which are economic and which may be readily adapted to production.

Since the completion of this work in 1941 articles dealing with other aspects of the subject have been published. Some of the more recent are given in references 2 and 3.

2. Shielding of the Electromagnetic Field

The electromagnetic field to be screened may be divided into three components, namely (1) the radiation field which can extend to a great distance, (2) the electric-induction field which falls off rapidly with distance, and (3) the magnetic-induction field which also falls off rapidly with distance. The relative magnitudes of these fields at any point depend upon the nature of the source. For sources which are amenable to analysis (e.g., the electric dipole and the

MS accepted by the Editor, February 1947.

loop) it is readily shown[4] that the three components of field have magnitudes of the same order at a distance of $r = \lambda_0/2\pi$, where λ_0 is the wavelength *in vacuo*. Where the receiver is located at a distance from the source appreciably greater than $\lambda_0/2\pi$, suppression may be achieved by shielding only the radiation field. This applies to all cases of v.h.f. interference in which the receiver is not located in the same vehicle as the source.

2.1. *Radiation Field*

The screening of a radiation field by a metallic enclosure is caused by the attenuation which occurs when the electromagnetic wave passes through the metal of the shield. It can be shown[4] that, for a plane wave, the attenuation factor R_r due to propagation through a homogeneous isotropic conducting screen is given by—

$$R_r = e^{-t/d} \qquad \ldots \quad \ldots \quad \ldots \quad (1)$$

where—

- t = thickness of the conducting screen.
- μ = magnetic permeability of the conductor.
- ρ = volume resistivity of the conductor.
- ω = $2\pi \times$ frequency.
- R_r = ratio of the amplitude of the wave upon leaving the conductor to its amplitude upon entering.

and $$d = \left(\frac{\rho}{2\pi\mu\omega}\right)^{\frac{1}{2}} \qquad \ldots \quad \ldots \quad \ldots \quad (2)$$

It may be shown[4] that the term d, which will be referred to as the "depth of penetration," is equal to the ratio of the volume resistivity to the surface resistivity of a plane semi-infinite conductor. The depth of penetration is a property of the material and may be greater than the actual thickness.

Thus it appears that the entire thickness of the shield is effective since the radiation field is attenuated progressively as it passes through the material of the shield. The attenuation depends only upon the ratio of the thickness to the depth of penetration. It should be noted that, if the shield does not completely enclose the source, part of the radiation will escape attenuation.

It is of interest to compare the calculated values of the attenuation for various metals, assuming that the volume resistivity is the same as the direct-current value. Thus the attenuations occurring in copper, aluminium and iron† at 50 Mc/s are found to be 1,000, 700 and 2,000 db/mm respectively.

†The figure for the attenuation in iron is based upon the value $\mu = 40$ given by Sutton in Ref. 5.

2.2. *Induction Field*

Where the receiver is located on the same vehicle as the source of interference, their separation may be less than $\lambda_0/2\pi$, and it becomes necessary to shield the induction fields as well as the radiation field. For a static electric field, perfect screening is possible by totally enclosing the source within a conductor since the potential must be the same at all points on the inner surface of the conductor. At v.h.f. the electric induction field may also be screened by enclosing the source within a conductor, but the screening is not then perfect since potential differences may be induced on the inner surface of the shield. The magnitude of these induced potential differences will depend primarily upon the ratio of the surface dimensions of the shield to the wavelength, and their penetration through the shield would appear to be related chiefly to the ratio of the thickness to the depth of penetration.

In a magnetic induction field the tangential component is attenuated exponentially and is negligible at depths substantially greater than d, the depth of penetration. The effect on the normal component of the field can be computed in simple cases by the assumption that the shield is thin or, more exactly, that the distribution of current across the thickness of the shield does not affect the distribution in the plane of the shield. Where the source and the receiver are parallel loops and the shield is a thin plane conducting sheet situated close to the source, it is shown in Appendix I that the screening factor due to the insertion of the sheet is given by—

$$R_m = \frac{\sigma\left\{\dfrac{a^2+b^2+c^2}{(a-b)^2+c^2}E - K\right\}}{2\pi\omega c\left\{1+\left(\dfrac{a+b}{c}\right)^2\right\}\left\{\dfrac{a^2+b^2+c^2}{(a+b)^2+c^2}K - E\right\}} \qquad \ldots \quad \ldots \quad \ldots \quad (3)$$

where—

- R_m = ratio of magnetic flux linking the receiving loop when the shield is in position to that when it is removed.
- ω = $2\pi \times$ frequency.
- c = distance between transmitting and receiving loops.
- a = radius of transmitting loop.
- b = radius of receiving loop.
- K, E = complete elliptic integrals of 1st and 2nd kinds respectively the parameter being a function of a, b, c as shown in Appendix I.

When c is greater than $a + b$, this relation approximates to—

$$R_m = \frac{3\sigma}{2\pi\omega c\left\{1 + \left(\frac{a-b}{c}\right)^2\right\}} \quad .. \quad (4)$$

Where the shield is a thin spherical shell enclosing the receiver and is located in a uniform field, it is shown in Appendix II that the screening factor due to the shield is given by—

$$R_m = \frac{3\sigma}{4\pi\omega a} \quad .. \quad .. \quad .. \quad (5)$$

where a = radius of shield.

In the above formulæ σ represents the effective surface resistivity with reference to the eddy currents. If the shield is infinitely thin, then—

$$\sigma = \rho/t$$

where t = thickness.

If, however, t is comparable with the depth of penetration d, then the effective resistivity is increased by skin effect. If $t > 2d$, then to a close approximation t may be replaced by d in the preceding equations, giving—

$$\left.\begin{aligned} \sigma &= (2\pi\omega\mu\rho)^{\frac{1}{2}} \\ \text{and—} \quad \sigma/2\pi\omega &= \mu d \end{aligned}\right\} \quad .. \quad (6)$$

Equations (3), (4) and (5) show that the screening factor for the magnetic induction field is a function only of the dimensions of the source and receiver, the separation of the receiver from the shield, the frequency and the surface resistivity of the shield. The screening factor is thus independent of the thickness of the shield when the latter is greater than twice the depth of penetration. Any thickness in excess of this value is redundant. Since the eddy currents flowing in the shield are confined to that part of its surface near the source, the shield does not require to enclose the source.

The efficacy of a sheet conductor as a shield thus varies inversely as the quantities d/t and $\sigma/2\pi\omega$ or μd (but d is a function of μ) which may be determined directly by observing the attenuation produced by interposing the sheet between transmitting and receiving loops, providing the test can be so arranged that the requisite field components are isolated. Since the magnetic induction field falls off with distance much more rapidly than the radiation component, the latter may readily be isolated by making measurements at a sufficient distance from the source. Some difficulty would, however, be encountered in attempting to isolate effectively a magnetic induction field at v.h.f. because of the small separations involved. There are, however, other methods available for measuring σ directly. In the resonance method, which is examined in the present paper, the sheet conductor, in the form of a washer, is coupled inductively to a resonant circuit. The loss introduced into the circuit by the washer is determined by observing the change in the width of the resonance curve, and from this loss the surface resistivity may be deduced. The method is suitable for frequencies up to 50 Mc/s. For frequencies above this a thermal method would be more suitable.

3. Experimental Details of Resonance Method

The test circuit, shown in Fig. 1, consisted of the coil L connected in parallel with a standard variable air capacitor C and a square-law valve voltmeter. The test coil was coupled through a Faraday screen to an intermediate circuit, which in turn was coupled with the oscillator. The intermediate circuit, which was introduced to filter out harmonics, was coupled sufficiently loosely with the test circuit to render the intermediate current constant.

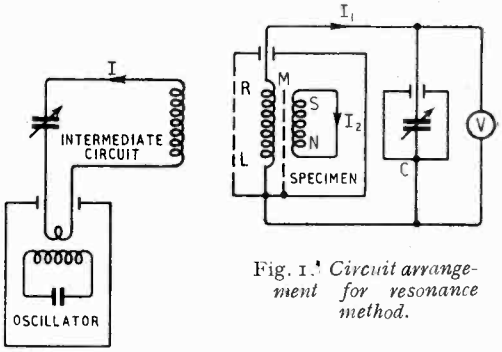

Fig. 1. *Circuit arrangement for resonance method.*

The specimens were in the form of washers which could be inserted in a Keramot holder mounted on the base of coil L and enclosed within the coil screen. The specimens were accurately located by the holder and, in some tests, were separated from the coil by a Faraday screen. The test circuit was adequately screened to prevent direct pick-up from the oscillator and external sources.

The oscillator was set to the required frequency and the intermediate circuit tuned to it. The resonance curve of the test circuit was then observed by varying

the capacitor C, thus giving the capacitance at resonance and the capacitance deviation at $1/\sqrt{2}$ of the maximum voltage reading. These observations were made in turn with (a) specimens, (b) standards and (c) no washer in the holder. In this way the specimens were compared with solid metal standards. The residual capacitance of the circuit was determined from the relation between capacitance and frequency.

4. Theory of Resonance Method

The effective series resistance of the test circuit is proportional to the width of its resonance curve as observed by varying the capacitance. When a specimen is coupled to the circuit, this resistance increases while the effective inductance falls. The resistance introduced into the circuit may be derived from the resulting change in the width of the resonance curve, while the inductance is determined by the change in the resonance point.

In order to derive the resistance of the specimen from the observations, it is necessary to make an analysis which includes the effects of mutual coupling between the test circuit, the specimen, and the intermediate circuit. It is shown in Appendix III that, provided all the coupling is inductive and the intermediate circuit coupling is adequately weak, the power factor of the specimen is given by the expression—

$$\frac{S}{\omega N} = \frac{C_r \delta C_0}{C_{0r}(C_r - C_{0r})}\left(\frac{C_{0r}^2 \delta C}{C_r^2 \delta C_0} - 1\right) \quad .. \quad (7)$$

where—

S = series resistance of the specimen.
N = self-inductance of the specimen.
ω = $2\pi \times$ frequency.
C_r, C_{0r} = capacitance of the test circuit at resonance with and without the specimen respectively.
δC, δC_0 = change in capacitance from the resonant value, with and without the specimen respectively, required to reduce the voltage across the capacitor to $1/\sqrt{2} \times$ voltage at resonance.

In order to determine S from Equ. (7), it is necessary to know the value of the specimen inductance N. If it is assumed that the specimen acts as a single circuit, then the value of N may be obtained by calculation as shown in Appendix IV. The expression is—

$$N = \frac{\pi}{2}(r_1 + r_2)\left[4\left\{\left(1 + \frac{m^2}{16}\right)\log\frac{16}{m} - 2\right\} + \mu\left(\frac{4Z}{xY}\right)\left\{1 - \frac{m^2}{8}\left(\log\frac{16}{m} - \frac{1}{3}\right)\right\}\right] \quad .. \quad (8)$$

where—

r_1, r_2 = inner and outer radii respectively of specimen or standard
t = thickness of specimen or standard.
μ = magnetic permeability of the material of specimen or standard
$m = \dfrac{r_2 - r_1 + t}{r_1 + r_2}$
$4Z/xY$ = factor representing the skin effect and defined in Appendix IV.

The above formula makes the following approximations which are justified if $r_2 - r_1$ is small:

(a) It is assumed that the current distribution is independent of radius.
(b) Third and higher powers of m are neglected.
(c) The value of the factor $(4Z/xY)$ is assumed to be equal to that for a ring of circular section.

The surface resistivity of the washer is defined as the resistance per unit square of its surface and is given to a sufficient degree of accuracy by Equ. (6). In the expression for the power factor of the washer, denoted by $S/\omega N$ in Equ. (7), the term S represents the resistance of an equivalent circuit possessing the same power loss as the washer, calculated on the basis of the same current distribution as that used to obtain the value of self-inductance N [see Equ. (8)].

Equating the loss in the equivalent circuit with that occurring in the washer—

$$S\left[\int_{r_1}^{r_2}\left(\frac{dI}{dr}\right)dr\right]^2 = 2\pi\sigma\int_{r_1}^{r_2} r\left(\frac{dI}{dr}\right)^2 dr \quad .. \quad (9)$$

where—

I = total current circulating inside any circle of radius r
r_1 and r_2 = inner and outer radii of the washer respectively.

The relation between S and σ can thus be derived if the current distribution in the washer is known. Assuming that the current distribution is uniform as in the derivation of the expression for N, the term dI/dr in Equ. (9) becomes a constant and the equation reduces to—

$$\frac{S}{\sigma} = \frac{\pi(r_2 + r_1)}{r_2 - r_1} \quad .. \quad .. \quad .. \quad (10)$$

Thus the relation between S and σ is a straight line passing through the origin with a slope dependent only upon the relative surface dimensions of the disc.

A straight-line relation, as obtained by testing suitable standards, may therefore be used to determine, by interpolation, the values of σ for the specimens. By using standards similar in dimensions and resistivity to the specimens under test, the inaccuracies due to errors in Equs. (8) and (10) and errors of interpolation can be reduced. For higher accuracy the specimens and the standards should be of simpler geometrical form (e.g., that of rings of circular section), so that the values of N and S may be more accurately calculated.

higher than that of Eureka (see Table II), it was considered desirable to include high surface resistivity standards. Hence the inclusion of iron and steel standards which, by virtue of their high magnetic permeability, have high surface resistivity [see Equ. (6)]. The employment of ferromagnetic discs as standards involves a knowledge of the permeability of the material at the test frequency. Previous tests[5] on specimens in the form of iron wire had yielded a value of $\mu = 40$ at the frequency of 50 Mc/s, and this figure was adopted.

TABLE I

List of Specimens and Standards

No.	Metal	Nature of Surface	Thickness (mm)	Diameter (cm) Inner	Diameter (cm) Outer	Calculated Surface Resistivity at 50 Mc/s, (mΩ)
	Standards:					
1	Copper 38 S.W.G.	Solid Washer	0.14	0.9	5.0	1.72
2	Aluminium 20 S.W.G.	,,	0.91	0.9	5.0	2.51
3	Zinc 21 S.W.G.	,,	0.76	0.9	5.0	3.47
4	Eureka 30 S.W.G.	,,	0.33	0.9	5.0	9.80
5	Iron 36 S.W.G.	,,	0.19	0.9	5.0	32.0
6	Copper	,,	3.3	1.3	7.6	1.72
7	Aluminium	,,	3.5	1.3	7.6	2.51
8	Eureka	,,	3.5	1.3	7.6	9.80
9	Steel	,,	3.2	1.3	7.6	32.0
10	Copper	,,	3.3	0.9	5.0	1.72
11	Aluminium	,,	3.5	0.9	5.0	2.51
12	Eureka	,,	3.5	0.9	5.0	9.80
13	Steel	,,	3.2	0.9	5.0	32.0
	Specimens:					
A	Copper on Commercial Zinc	Sprayed on Plastic	—	0.9	5.0	—
B	Pure Zinc	,,	0.16*	0.9	5.0	—
C	Commercial Zinc ..	,,	0.03*	0.9	5.0	—
D	Copper	Electrodeposited on Steel	3.3†	1.3	7.6	—
E	Nickel	,,	3.2†	1.3	7.6	—

* Thickness of sprayed metal only. † Total thickness of the specimen including the base.

5. Results of Tests

Two groups of specimens were tested, namely, (a) washers consisting of copper and zinc sprayed upon a plastic base, and (b) washers consisting of copper and nickel electrodeposited upon a steel base. More complete data relating to the specimens are given in Table I, which also includes properties of the standards employed. It will be seen that the standards were similar in dimensions to the specimens and were made from metals possessing a wide range of resistivity. Since the sprayed-metal specimens were found to have a surface resistivity

TABLE II

Specimens of Metallic Surfaces Arranged in Order of Measured Surface Resistivity at 50 Mc/s.

Copper, Copper-plated steel
Nickel-plated steel, Eureka
Sprayed pure zinc
Sprayed copper on sprayed commercial zinc
Iron or steel
Sprayed commercial zinc

Since the values obtained for S are dependent upon N, it is essential, for ferromagnetic specimens or standards, to determine to what extent the permeability affects N. It can be shown that, for the conditions of the test,

the second term of Equ. (8), which represents the contribution due to permeability, does not exceed 1 per cent of the total. This is because the depth of penetration is so small that only a negligible part of the magnetic flux passes through the disc. Hence the inductance of the ferromagnetic discs is independent of their permeability.

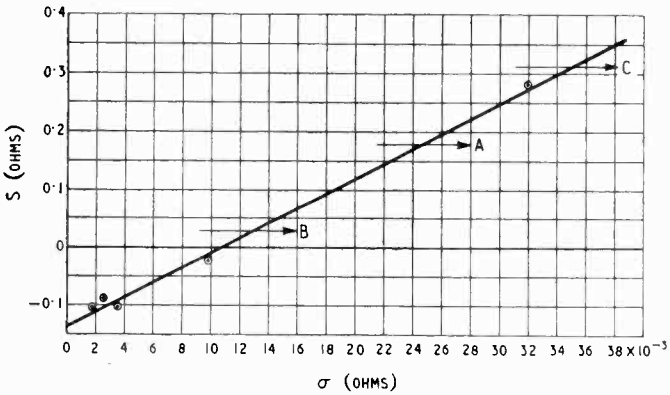

Fig. 2 (above). *Comparison of sprayed specimens with thin sheet standards without screening.*

Fig. 3 (right). *Comparison of electroplated specimens with solid metal standards with electrostatic screening.*

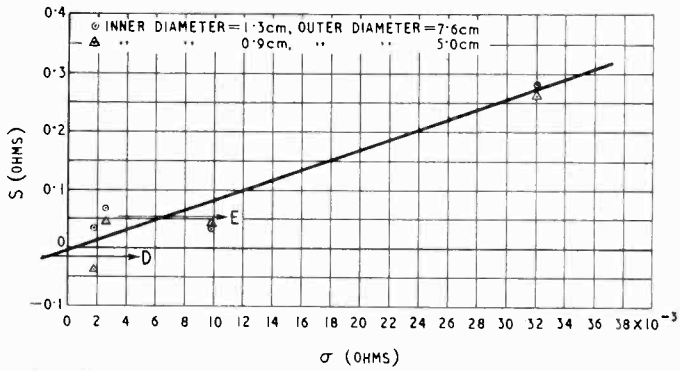

The results of the experimental comparison between the sprayed metal specimens A, B, C and the standards 1–5 are shown in Fig. 2, while those for the comparison between the electrodeposited specimens D, E and the standards 6–13 are shown in Fig. 3. These results confirm the theory in that the relation between S and σ is linear. It is, however, seen that in Fig. 2 the line does not pass through the origin. This is probably due to the fact that the tests on sprayed specimens were conducted without screening the disc from the test circuit, thus permitting capacitive coupling which was disregarded in the theory. Introduction of a Faraday screen in the tests on electrodeposited specimens makes the line pass more nearly through the origin. It is seen in Fig. 3 that points representing discs of different radii but similar proportions fall on the same straight line, thus confirming the theoretical deduction that the ratio S/σ is independent of the radius of the disc, providing the ratio of outer to inner radius is constant.

In Fig. 4 the relation between d.c. resistance and v.h.f. resistance of the sprayed specimens is seen to be linear, indicating that the maximum depth of penetration was not reached. The direct-current resistance values were higher than those calculated from the volume resistivity of the metal. Thus it appears that the volume resistivity of the metals was increased on spraying, probably by virtue of oxide inclusions.

The accuracy of the present tests does not appear to justify the presentation of results in greater detail than is shown in Table II, where specimen and standard materials are arranged in order of surface resistivity.

6. Conclusions

The following conclusions have been drawn from the experimental results and the theoretical treatment:

1. When a conducting sheet is used to shield from a radiation field, its efficacy is determined by the ratio of its thickness to the depth of penetration. A high value of this ratio is readily obtained at very high frequencies, and it is thus relatively easy to screen a receiver against radiation. To be effective the shield should completely separate the source from the receiver.

2. When the separation between the source and the receiver is small, the magnetic induction field predominates and the efficacy of a shield is then determined by the inverse of the product of its magnetic permeability and its depth of penetration; i.e., the ratio of its effective surface resistivity to frequency.

3. The surface resistivity of copper and

nickel is shown not to be greatly altered by electrodepositing on a steel base.

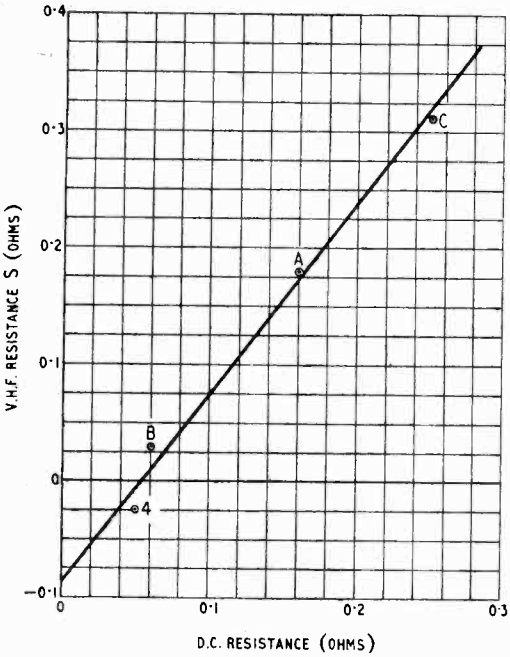

Fig. 4. *Relation between v.h.f. and d.c. resistance of sprayed specimens.*

4. The resistivity of copper and zinc is increased to values higher than that of Eureka by spraying on a plastic base. Since the value of v.h.f. resistivity is only slightly greater than that of direct-current resistivity in the latter case, the effect is probably due to oxide inclusions and requires further investigation. This may be made by testing sprayed coatings of various thicknesses at several frequencies in order to determine whether oxide formed during spraying merely increases the volume resistivity of a specimen or introduces stratification.

5. Use of specimens and standards of simpler geometrical form would permit a more accurate evaluation of the inductance N and of the ratio of the resistance S to the resistivity σ. Further, to make the results more reliable, more standards covering the high-resistivity range are needed, thus enabling a more detailed examination of sprayed specimens to be undertaken.

6. The extent to which the magnetic permeability of a ferromagnetic disc affects its inductance N is shown to be less than 1 per cent at 50 Mc/s.

7. Acknowledgments

The author wishes to acknowledge his indebtedness to Dr. S. Whitehead, Director of the British Electrical and Allied Industries Research Association and to Dr. G. Mole of the Association Staff for their valuable suggestions in connection with the work described.

He also wishes to thank Dr. Whitehead and the Ministry of Supply for permission to publish the paper.

APPENDIX I

Shielding of a Circular Coil by a Thin Conducting Sheet.

Let—

a = radius of sending loop.

b = radius of receiving loop.

c = axial separation of the loops.

r, z, ϕ = cylindrical co-ordinates of any point with respect to centre of sending loop as origin.

t = time.

$I \cos \omega t$ = current in sending loop.

$k = \left[4ar \Big/ \left\{(a+r)^2 + z^2\right\}\right]^{\frac{1}{2}}$

$K = K(k)$ = complete elliptic integral of first kind.

$E = E(k)$ = complete elliptic integral of second kind.

ω = $2\pi \times$ frequency.

σ = effective surface resistivity of shield.

N = flux through receiving loop in absence of shield.

N' = flux through receiving loop due to eddy currents in shield.

It can be shown[4] that—

$$N = 4\pi a r I \cos \omega t \int_0^{\pi} \frac{\cos \phi \, d\phi}{(a^2 + r^2 - 2ar \cos \phi + z^2)^{\frac{1}{2}}} \qquad (11)$$

$$= \frac{8\pi I \cos \omega t}{k} \sqrt{ar} \left\{\left(1 - \frac{1}{2}k^2\right) K - E\right\}$$

By Maxwell's method of images for a plane conducting sheet (located close to the sending loop)—

$$N' = \int_0^{\infty} \frac{\partial}{\partial t} N\left(t - u, z + \frac{\sigma u}{2\pi}\right) du$$

$$= 4\pi r a \omega I \int_0^{\pi} \cos \phi \left[\int_0^{\infty} \frac{\sin \omega(t-u)\, du}{\left\{a^2 + r^2 - 2\,ar \cos \phi + \left(z + \frac{\sigma u}{2\pi}\right)^2\right\}^{\frac{1}{2}}}\right] d\phi \qquad (12)$$

If ω is large, the series for an integral of a product may be used giving—

$$N' = 4\pi r a I \int_0^{\pi} \left[\frac{-\cos \omega t \cos \phi \, d\phi}{(a^2 + r^2 - 2ar \cos \phi + z^2)^{\frac{1}{2}}} + \frac{\sigma z \sin \omega t \cos \phi \, d\phi}{2\pi\omega (a^2 + r^2 - 2ar \cos \phi + z^2)^{\frac{3}{2}}} \right]$$

$$= -\left(N + \frac{\sigma}{2\pi\omega} \frac{\partial N}{\partial z} \tan \omega t \right) \quad .. \quad (13)$$

Thus, if the screening factor R_m is defined as the ratio of flux linkage through receiving loop with the shield in position to that without the shield, then—

$$R_m = \frac{|N + N'|}{|N|} = \frac{\sigma}{2\pi\omega} \left| \frac{1}{N} \frac{\partial N}{\partial z} \right|$$

Substituting for N, and putting $r = b$, $z = c$,

$$R_m = \frac{\sigma c \left\{ -K + \frac{a^2 + b^2 + c^2}{(a-b)^2 + c^2} E \right\}}{2\pi\omega \left\{ (a+b)^2 + c^2 \right\} \left\{ \frac{a^2 + b^2 + c^2}{(a+b)^2 + c^2} K - E \right\}} \quad .. \quad .. \quad (14)$$

The functions K and E are tabulated[6] whence R_m may be calculated.

If $k < 0.5$, then to 1 per cent—

$$K = \frac{\pi}{2}\left(1 + \frac{k^2}{4}\right)$$

$$E = \frac{\pi}{2}\left(1 - \frac{k^2}{4}\right)$$

and—

$$R_m = \frac{3\sigma}{2\pi\omega c \left\{ 1 + \left(\frac{a-b}{c} \right)^2 \right\}} \quad .. \quad .. \quad (15)$$

APPENDIX II

Shielding by a Thin Spherical Conducting Shell.

In this case the field before and after the introduction of the shield can usually be expanded as a convergent series of spherical harmonics if axially symmetrical, and it has been shown[4] that the ratio R_{mn} of the nth term of the field inside the shell to that with the shield removed is—

$$R_{mn} = \sin\left[\tan^{-1} \frac{(2n+1)\sigma}{4\pi a \omega} \right] \quad .. \quad .. \quad (16)$$

where a = radius of shell, and σ and ω have the same meaning as in Appendix I.

The value to be adopted depends on the rate of convergence and nature of the series which expresses the original field but usually a sufficiently representative value is obtained by considering only one or two terms. For a uniform field $n = 1$, and

$$R_m = \frac{3\sigma}{4\pi a \omega} \quad .. \quad .. \quad .. \quad (17)$$

if R_m is small.

APPENDIX III

Circuit Analysis for Resonance Method.

A circuit analysis which includes the effects of mutual inductive coupling between the test circuit, the specimen, and the intermediate circuit (see Fig. 1) may be made in the following manner :—

Let—

R = series resistance of the test circuit.

L = self inductance of the test circuit.

S = series resistance of the specimen.

N = self inductance of the specimen.

M = mutual inductance between the specimen and the test circuit.

M_1 = mutual inductance between the intermediate circuit and the test circuit.

M_2 = mutual inductance between the intermediate circuit and the specimen.

I_1 = current in the test circuit.

I_2 = current in the specimen.

I = current in the intermediate circuit.

V = potential developed across the capacitor.

C = capacitance of the test circuit with the specimen coupled.

C_0 = capacitance of the test circuit without the specimen coupled.

C_r = capacitance of the test circuit at resonance with the specimen coupled.

C_{0r} = capacitance of the test circuit at resonance without the specimen coupled.

δC = change in capacitance, from the resonant value with the specimen coupled, required to reduce the voltage across the capacitor to $1/\sqrt{2} \times$ voltage at resonance.

δC_0 = change in capacitance, from the resonant value without the specimen coupled, required to reduce the voltage across the capacitor to $1/\sqrt{2} \times$ voltage at resonance.

The three circuital relations are—

$$I_1 = j\omega C V \quad .. \quad .. \quad (18)$$

$$j\omega M_1 I + j\omega M I_2 = \left\{ R + j\left(\omega L - \frac{1}{\omega C} \right) \right\} I_1 \quad (19)$$

and—

$$j\omega M_2 I + j\omega M I_1 = (S + j\omega N) I_2 \quad .. \quad (20)$$

On eliminating I_1, these equations reduce to—

$$M_1 I + M I_2 = \left\{ R + j\left(\omega L - \frac{1}{\omega C} \right) \right\} C V \quad (20.1)$$

and—

$$j\omega M_2 I - \omega^2 M C V = (S + j\omega N) I_2 \quad .. \quad (20.2)$$

which may be combined to eliminate I_2 as follows :—

$$\left\{ M_1 (S + j\omega N) + j\omega M M_2 \right\} I = C V \left[\omega^2 M^2 + \left\{ R + j\left(\omega L - \frac{1}{\omega C} \right) \right\} \left(S + j\omega N \right) \right] \quad .. \quad (21)$$

When the specimen is removed, $M = M_2 = 0$, C and V become C_0 and V_0 respectively, and I remains constant. Equ. (20.1) then becomes—

$$M_1 I = C_0 V_0 \left\{ R + j\left(\omega L - \frac{1}{\omega C_0} \right) \right\} \quad .. \quad (22)$$

whence I is eliminated by combining with Equation (21)—

$$\frac{CV}{C_0 V_0} = \frac{\left\{ R + j\left(\omega L - \frac{1}{\omega C_0} \right) \right\} \left\{ S + j\omega N + j\omega M \frac{M_2}{M_1} \right\}}{\omega^2 M^2 + \left\{ R + j\left(\omega L - \frac{1}{\omega C} \right) \right\} (S + j\omega N)} \quad .. \quad .. \quad .. \quad .. \quad .. \quad (23)$$

The value of L can be derived from Equ. (22) in terms of C_{0r}, which is the particular value of C_0 at resonance with the specimen removed (or corresponding to the maximum value of V_0). Thus— $L = \frac{1}{\omega^2 C_{0r}}$ and this may be substituted in Equ. (23) as follows— .. .. (24)

$$\frac{CV}{C_0 V_0} = \frac{\left\{R + j\left(\frac{1}{\omega C_{0r}} - \frac{1}{\omega C_0}\right)\right\}\left\{S + j\omega N\left(1 + \frac{M}{N}\frac{M_2}{M_1}\right)\right\}}{\omega^2 M^2 + \left\{R + j\left(\frac{1}{\omega C_{0r}} - \frac{1}{\omega C}\right)\right\}\left\{S + j\omega N\right\}} \quad \text{.. .. .. (25)}$$

At resonance with the specimen coupled, C, V, C_0, V_0 become C_r, V_r, C_{0r}, V_{0r} respectively, and Equation (25) becomes—

$$\frac{C_r V_r}{C_{0r} V_{0r}} = \frac{R\left\{S + j\omega N\left(1 + \frac{M}{N}\frac{M_2}{M_1}\right)\right\}}{\omega^2 M^2 + \left\{R + j\left(\frac{1}{\omega C_{0r}} - \frac{1}{\omega C_r}\right)\right\}(S + j\omega N)} \quad \text{.. .. .. (26)}$$

Combining Equs. (25) and (26)—

$$\frac{CV\,C_{0r}V_{0r}}{C_r V_r C_0 V_0} = \frac{\left\{R + j\left(\frac{1}{\omega C_{0r}} - \frac{1}{\omega C_0}\right)\right\}\left[\omega^2 M^2 + \left\{R + j\left(\frac{1}{\omega C_{0r}} - \frac{1}{\omega C_r}\right)\right\}(S + j\omega N)\right]}{R\left[\omega^2 M^2 + \left\{R + j\left(\frac{1}{\omega C_{0r}} - \frac{1}{\omega C}\right)\right\}(S + j\omega N)\right]} \quad \text{.. .. (27)}$$

Let— $C = C_r \pm \delta C$

and— $C_0 = C_{0r} \pm \delta C_0$

By definition— $\frac{V_r}{V} = \frac{V_{0r}}{V_0} = \sqrt{2}$

Equ. (27) now becomes—

$$\left(1 \pm \frac{\delta C}{C_r} \pm \frac{\delta C_0}{C_{0r}}\right) R\left[\omega^2 M^2 + \left\{R + j\left(\frac{1}{\omega C_{0r}} - \frac{1}{\omega C}\right)\right\}(S + j\omega N)\right]$$
$$= \left\{R + j\left(\frac{1}{\omega C_{0r}} - \frac{1}{\omega C_0}\right)\right\}\left[\omega^2 M^2 + \left\{R + j\left(\frac{1}{\omega C_{0r}} - \frac{1}{\omega C_r}\right)\right\}(S + j\omega N\right] \quad \text{.. .. .. (28)}$$

Neglecting $\delta C/C_r$ and $\delta C_0/C_{0r}$ in comparison with unity, Equ. (28) reduces to—

$$R\left(\frac{C_{0r}^2\,\delta C}{C_r^2\,\delta C_0} - 1\right) = \frac{\omega^2 M^2}{S^2 + \omega^2 N^2}(S - j\omega N) + \frac{j\omega(C_r - C_{0r})}{\omega^2 C_r C_{0r}} \quad \text{.. .. .. (29)}$$

The real and imaginary parts of Equ. (29) respectively give—

$$\frac{\omega^2 M^2}{S + \omega^2 N^2} = \frac{R}{S}\left(\frac{C_{0r}^2\,\delta C}{C_r^2\,\delta C_0} - 1\right) \quad \text{.. (30)}$$

and—

$$\frac{\omega^2 M^2}{S^2 + \omega^2 N^2} = \frac{C_r - C_{0r}}{\omega N\,\omega C_r C_{0r}} \quad \text{.. .. (31)}$$

Whence, eliminating M—

$$\frac{S}{\omega N R} = \frac{\omega C_r C_{0r}}{C_r - C_{0r}}\left(\frac{C_{0r}^2\delta C}{C_r^2\delta C_0} - 1\right) \quad \text{.. .. (32)}$$

It is known that—

$$R = \frac{\delta C_0}{\omega C_{0r}^2} \quad \text{.. .. .. .. (33)}$$

Substituting for R in Equ. (32)—

$$\frac{S}{\omega N} = \frac{C_r \delta C_0}{C_{0r}(C_r - C_{0r})}\left(\frac{C_{0r}^2\delta C}{C_r^2\delta C_0} - 1\right) \quad \text{.. (34)}$$

APPENDIX IV

Derivation of Self-Inductance of Washer

An expression for the self-inductance of the washer may be derived in the following way by assuming it to be equivalent to a circular ring of elliptical cross-section :—

Let—

N = self-inductance of the washer with uniform surface distribution of current.

r_1 = inner radius.

r_2 = outer radius.

t = thickness.

$m = \frac{r_2 - r_1 + t}{r_1 + r_2}$

$x = \frac{r_2 - r_1 + t}{2}\sqrt{\frac{\pi\omega\mu}{\rho}}$

μ = magnetic permeability of the material.

ρ = volume resistivity of the material.

ω = $2\pi \times$ frequency.

$Y = (\text{ber}'x)^2 + (\text{bei}'x)^2$

$Z = \text{ber}\,x\,\text{ber}'x + \text{bei}\,x\,\text{bei}'\,x$.

ber x = the real component of the Bessel function of order zero, J_0, having for its argument $xj\sqrt{j}$ where x is a real quantity and $j = \sqrt{-1}$.

bei x = the imaginary component of the above Bessel function.

ber$'\,x = d\,(\text{ber}\,x)/dx$

bei$'\,x = d\,(\text{bei}\,x)dx$.

The following formula[7] for the self-inductance of a non-magnetic circular ring with circular cross-section was derived by Rayleigh, Wien and Teresawa :—

$$L_s = 4\pi a\left[\left(1 + \frac{b^2}{8a^2}\right)\log\frac{8a}{b} + \frac{b^2}{24a^2} - 1.75\right] \quad (35)$$

where—

a = mean radius of the ring.
b = radius of the cross-section.
L_s = self-inductance of the ring.

In the above formula, third and higher powers of b/a are neglected and a uniform surface distribution of current is assumed. Grover employed Wien's method to obtain, with the same approximations as above, the following expression for the self-inductance L_0 of a circular ring with cross-section consisting of a circular line—

$$L_0 = 4\pi a\left[\left(1 + \frac{b^2}{4a^2}\right)\log\frac{8a}{b} - 2\right] \quad .. \quad .. \quad (36)$$

L_s in Equ. (35) represents the self-inductance due to the total magnetic flux in a non-magnetic ring, while L_0 in Equ. (36) represents the component of self-inductance contributed by the flux located outside the ring. Combining Equs. (35) and (36)—

$$L_s - L_0 = \pi a\left[1 - \frac{b^2}{2a^2}\left(\log\frac{8a}{b} - \frac{1}{3}\right)\right] \quad .. \quad (37)$$

For a ferro-magnetic material, this component of the self-inductance is given by—

$$\mu\,(L_s - L_0) = \mu\pi a\left[1 - \frac{b^2}{2a^2}\left(\log\frac{8a}{b} - \frac{1}{3}\right)\right]$$

At high frequencies the flux in the ring is confined to its surface by virtue of skin effect. This is taken into account by the factor $(4Z/xY)$, where $x = 2b\sqrt{\pi\omega\mu\rho}$ and the inside component of the self-inductance becomes—

$$\mu\left(\frac{4Z}{xY}\right)(L_s - L_0) = \mu\left(\frac{4Z}{xY}\right)\pi a \left[1 - \frac{b^2}{2a^2}\left(\log\frac{8a}{b} - \frac{1}{3}\right)\right] \quad .. \quad (38)$$

Thus, the total self-inductance of the ring is—

$$L = L_0 + \mu\left(\frac{4Z}{xY}\right)(L_s - L_0)$$
$$= 4\pi a\left[1 + \frac{b^2}{4a^2}\left(\log\frac{8a}{b} - 2\right)\right] + \mu\left(\frac{4Z}{xY}\right)\pi a\left[1 - \frac{b^2}{2a^2}\left(\log\frac{8a}{b} - \frac{1}{3}\right)\right] \quad (39)$$

According to the treatment adopted by Rosa and Grover, the above formula may be used in the case of a circular ring of elliptical cross-section by making—

$$b = \frac{\alpha + \beta}{2} \quad .. \quad .. \quad .. \quad .. \quad (40)$$

where α and β are the principal semi-axes of the cross-section, since the geometrical mean distances are then identical.[7] A washer may be assumed to be approximately a ring of elliptical cross-section, such that—

$$\alpha = \frac{r_2 - r_1}{2}$$

$$\beta = \frac{t}{2}$$

and—

$$a = \frac{r_1 + r_2}{2}$$

Thus, the values of x as defined in the cases of elliptical and circular sections are identical, provided $b = (r_2 - r_1 + t)/4$. Substituting for the values of a and b in Equ. (39),

$$N = \frac{\pi}{2}(r_1 + r_2)\left[4\left\{\left(1 + \frac{m^2}{16}\right)\log\frac{16}{m} - 2\right\} + \mu\left(\frac{4Z}{xY}\right)\left\{1 - \frac{m^2}{8}\left(\log\frac{16}{m} - \frac{1}{3}\right)\right\}\right] \quad .. \quad (41)$$

REFERENCES

[1] Gill and Whitehead, *J. Instn elect. Engrs*, September 1938, Vol. 83, Part III, p. 345.

[2] C. F. Davidson, R. C. Looser and J. C. Simmonds, *Wireless Engineer*, January 1946, Vol. 23, p. 8.

[3] C. C. Eaglesfield, *Electronic Engineering*, Vol. 18, p. 106.

[4] W. R. Smythe "Static and Dynamic Electricity."

[5] E.R.A. Report Ref. M/T69.

[6] Jahnke and Emde, "Funktionentafeln."

[7] Rosa and Grover, Bureau of Standards, Sc. paper No. 169, Vol. 8, December 18th, 1916.

BOOKS RECEIVED

F.M. Simplified

By MILTON S. KIVER. Pp. 359 + vii, with 243 illustrations. Macmillan & Co. Ltd., St. Martin's St., London, W.C.2. Price 33s.

This book provides a simple explanation of the principles of frequency modulation and describes the apparatus needed for both transmission and reception.

Elements of Electrical Engineering.

By WALTER J. CREAMER. Pp. 344 + ix, with 260 illustrations. McGraw Hill Publishing Co. Ltd., Aldwych House, London, W.C.2. Price 24s. (in U.K.).

Applied Electronics

By D. HYLTON THOMAS, M.Sc.(Tech.), B.Sc. (Eng.) A.M.I.E.E., A.M.I.R.E. Pp. 131 + xi, with 90 illustrations. Blackie & Son, Ltd., 66, Chandos Place, London, W.C.2. Price 7s. 6d.

Television Simply Explained

By R. W. HALLOWS. Pp. 198, with 97 illustrations and 16 plates. Chapman & Hall, Ltd., 37, Essex St., London, W.C.2. Price 9s. 6d.

Standard Valves

Standard Telephones & Cables Ltd., Connaught House, Aldwych, London, W.C.2. Price 15s. 6d. (post free).

This handbook gives characteristics of the Standard range of valves:—repeater triodes, transmitting types, velocity modulation tubes, c.r. tubes and x-ray tubes. Broadcast receiving valves are not included.

One Story of Radar

By A. P. ROWE. Pp. 208 + xii, with 7 illustrations. Cambridge University Press, Bentley House, 200, Euston Rd., London, N.W.1. Price 8s. 6d.

This is a non-technical history of the Telecommunications Research Establishment from 1934 to the end of the war by one who was for some years its chief superintendent.

Cathode-Ray Oscillographs.

By. J. H. REYNER. Pp. 189 + x, with 134 illustrations. Sir Isaac Pitman & Sons, Ltd., Kingsway, London, W.C.2. Price 8s. 6d.

STABLE VOLTMETER AMPLIFIER

By J. D. Clare, M.Sc.(Eng.), A.M.I.E.E.

(*Research Dept., R.F. Equipment Limited, Hirwun, Glamorgan*).

SUMMARY.—An analysis is given of a d.c. amplifier circuit suitable for use as an electrostatic d.c. voltmeter and also with a diode probe, as a peak-reading a.c. voltmeter.

The meter reading is shown to be independent of changes in h.t. voltage and effectively independent of changes in the valve parameters.

1. Introduction

IN all multi-range a.c. voltmeters using the normal peak-reading diode head, a d.c. amplifier is necessary in order to obtain a usable value of meter current for low input voltages with a high input impedance.

The required characteristics of such an amplifier can be summarized as follows :—

(a) The "zero set" should not alter as the voltage range is changed.

(b) The "zero set" should be independent of supply voltage variations.

(c) The meter reading for a given input voltage should be independent of valve parameters.

(d) The reading should also be independent of supply-voltage variations.

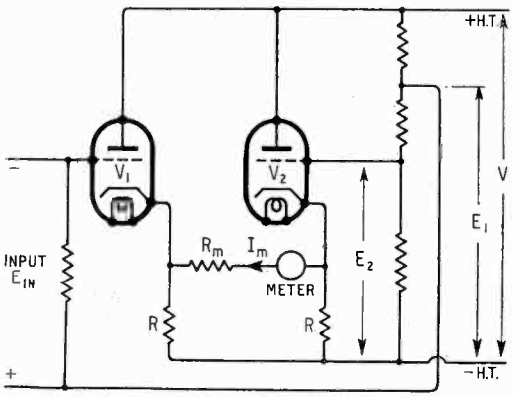

Fig. 1. *Basic circuit of the voltmeter amplifier.*

The circuit described reduces the effect of changes in supply voltage to a negligible factor without resorting to a stabilized power supply, and also meets the other conditions numbered above.

It is very desirable that the same amplifier should be suitable for measuring unidirectional voltages with a very high input impedance. This requirement is necessary if accurate measurements are to be made across such high impedance circuits as a.v.c. circuits in radio receivers.

MS accepted by the Editor, March 1947.

The required characteristics for the amplifier in this case are exactly the same as those enumerated previously for the a.c. voltmeter.

2. Basic Circuit

The basic circuit of the amplifier is shown in Fig. 1.

The input is either a unidirectional voltage applied in the polarity as shown to make the input grid negative, or it is the rectified output voltage from an a.c. peak reading diode head.

The current I_m through the meter, for an input unidirectional voltage of E_{IN} is shown in Appendix 1 to be

$$\frac{E_{IN}}{R_m + \frac{1}{g_{m1}} + \frac{1}{g_{m2}}}$$

It can be seen from this expression that the meter current I_m for a given input voltage E_{IN} is independent of the h.t. voltage V. This assumes, of course, that the change in anode volts across V_1 as represented by the change from O to Y in Fig. 5 is not large enough to cut off the anode current.

3. Valve Parameters

There remain only the terms g_{m1} and g_{m2} to be considered. Let us consider a practical example where V_1 and V_2 are two triodes type VR55 (Mullard EBC33) and R is 100 kΩ. With no input the anode current is 3.0 mA. This corresponds to the point O in Fig. 5. When an input voltage is applied, the operating conditions correspond to the point Y in Fig. 5. the valve V_1 having an anode current of I_1. The maximum value of I_m, that is the value of the meter current for full scale deflection, must be kept small compared with I_1. Hence, in this case, I_m is made either 100 μA or 200 μA for full scale deflection.

At the operating point chosen, the manufacturers' curves show $g_m = 1.0$ mA/V.

For widely different values of E_{IN} or R_m, the calculated meter current is compared with the measured current in Table I.

TABLE I

E_{IN} (V)	R_m (kΩ)	$R_m + 2/g_m$ (kΩ)	I_m (calculated) (μA)	I_m (measured) (μA)
1.5	5.2	7.2	208	210
3	27.45	29.45	100	100.5
120	600	602	200	200

For large values of input voltage, and therefore of R_m, the terms $\frac{1}{g_{m1}} + \frac{1}{g_{m2}}$ can be ignored and $I_m \approx \frac{E_{IN}}{R_m}$.

It is only for low values of input voltage E_{IN} that the effect of variation in g_m from valve to valve, and with ageing of the valves, need be considered.

Allowing for a 10% change in g_m the worst change in $\frac{2}{g_m}$ will be 10% of 2,000 ohms = 200 ohms.

For E_{IN} = 3 volts
I_m = 100 μA
$R_m + 2/g_m \approx 30$ kΩ for full scale deflection of 100 μA.

The 200-ohms change in $R_m + 2/g_m$ corresponds to less than 0.1% error in I_m.

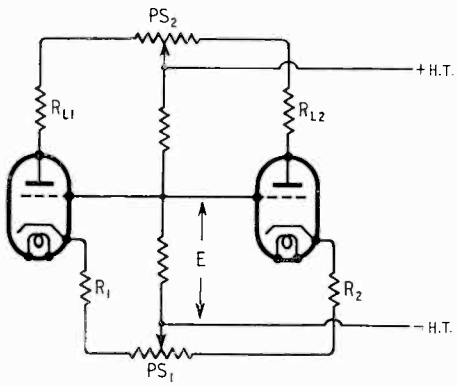

Fig. 2. *Insensitivity to h.t. voltage changes is achieved by the adjustment of PS_1 and PS_2.*

Hence by switching the value of R_m, it is possible to obtain a multi-range meter with the accuracy of reading determined by the accuracy of R_m and of the meter in series with it.

The circuit fulfils the conditions that the meter reading should be independent of h.t. voltage and should provide a zero-set that does not change from range to range.

It is still necessary to make the zero-set independent of h.t. changes or else an initial error, introduced if the meter does not read zero when there is no input voltage, is added to the normal meter reading for any finite input voltage.

4. Stability of Zero Set

If the two valves are initially balanced and then the h.t. voltage changes, there will obviously be a slight potential difference between the two cathodes unless the mutual conductances of both valves are identical. This will give rise to a current through the meter. It is obviously necessary to know how important this factor can be, allowing for the normal production variations in valve characteristics.

It is shown in Appendix 2 that for the circuit of Fig. 2 after initially balancing the valve with an h.t. voltage V so that there is no potential difference between the two cathodes, the potential between the two cathodes is

$$\Delta V \left\{ \frac{1}{\frac{r_{a1} + 2R_{L1}}{R_1(1 + k\mu_1)} + \frac{1}{k}} - \frac{1}{\frac{r_{a2} + 2R_{L2}}{R_2(1 + k\mu_2)} + \frac{1}{k}} \right\}$$

when the h.t. voltage changes to $V + \Delta V$ for this to be zero

$$\frac{r_{a1} + 2R_{L1}}{R_1((1 + k\mu_1)} = \frac{r_{a2} + 2R_{L2}}{R_2(1 + k\mu_2)}$$

As r_{a1}, r_{a2}, μ_1 and μ_2 can vary within limits of say ± 10 per cent, it is necessary to be able to control the values of R_{L1}, R_{L2}, R_1 and R_2 to make (17) become an identity.

This condition is achieved by use of the two pre-set potentiometers PS_1 and PS_2. The pre-set PS_1 controls the relative values of R_1 and R_2 and the pre-set PS_2 controls the relative values of R_{L1} and R_{L2}.

Using this circuit it is possible, on all ranges, to reduce the effect of mains variations to a negligible amount, without having to resort to a stabilized power supply.

5. Applications

For use as an electrostatic voltmeter the circuit of Fig. 3 may be used.

As already described R_m can be switched to provide various ranges. The input voltage is applied to the input terminals and a reading is obtained with an input resistance R_L.

On pressing the push-button P.B. the input grid then has a d.c. leakage path to cathode, through the source impedance across which the voltage is being measured. The reading is taken with an effectively infinite input impedance to direct current. As the source

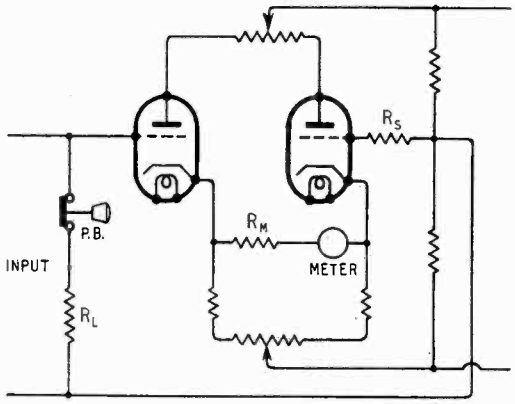

Fig. 3. *Practical circuit for voltage measurement.*

impedance is likely to vary over a very large range, it is important to use valves which give no trouble due to grid current. Using two VR.55 valves and making R_s equal to 1 MΩ, it is possible to measure the potential across source impedances varying from 0 to 15 MΩ without any noticeable inaccuracy due to grid current.,

This measurement is, of course, helped by making the input grid negative. The effective negative bias voltage of the grid of V_1 relative to its cathode increases slightly although the change is quite small.

When used in conjunction with a diode head, the meter can be calibrated to read various ranges of r.m.s. volts by switching in different values of R_m. The meter is then a normal peak-reading valve voltmeter with a consequent waveform error if the input is not a pure sine wave.

6. Range Extension

On all a.c. and d.c. ranges it is, of course, possible to extend the range by use of a resistance potential divider on the input while for a.c. measurements a capacitance potential divider may be employed. As very high resistance values are often required for this, particularly on the d.c. ranges, it was not incorporated in the instrument itself because of the instability and high tolerance on carbon-type resistors of very high value.

7. Meter Protection Device

When the meter is set on one of the low-voltage ranges, it can be overloaded and on d.c., the input voltage can be applied the wrong way round causing over-loading in the reverse direction.

As a protection against this, the circuit shown diagrammatically in Fig. 4 is used.

A twin-triode (6SN7) is connected as shown with common cathodes and a double-wound relay $\frac{C}{2}$ in the anode circuits.

With no input and with the valves balanced no current flows through R_{M1} and R_{M2} and hence the two grids of the twin-triode are at the same potential. The two anode currents are thus approximately equal and the relay is not operated.

If current flows in R_m in either direction, the anode currents of the twin triode go out

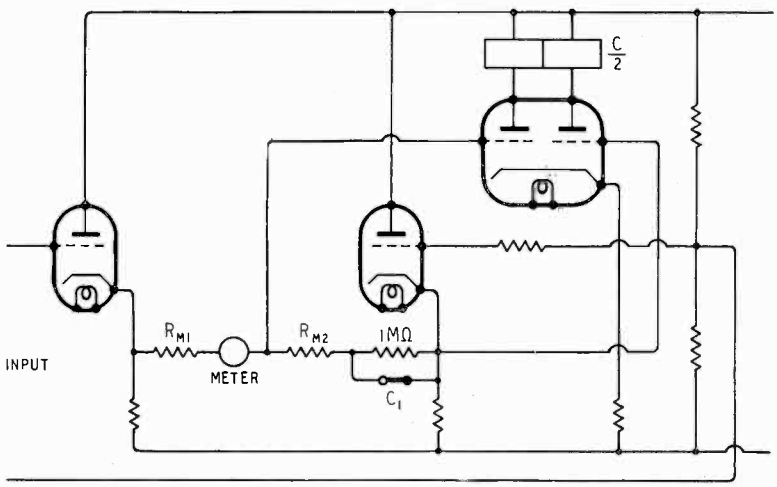

Fig. 4. *The use of a relay as an overload protection is shown here.*

of balance. The circuit can be so designed as to make the relay operate on a given meter current, say 200 per cent overload.

When the relay operates, the contact C_1 opens and the 1-MΩ resistance is then in

series with the meter. Another contact can be used to cause an alarm lamp to light up. This works for a current flowing in either direction and so gives protection against normal overload, and incorrect polarity of input on the d.c. ranges. The circuit also has the advantage that the sum of the two anode currents in the twin-triode remains substantially constant and so a constant drain is taken from the h.t. supply.

APPENDIX I

In the analysis of the circuit shown in Fig. 1 the following symbols are used :

g_{m1} = Mutual conductance of valve V_1.
g_{m2} = Mutual conductance of valve V_2.
r_{a1} = Internal resistance of valve V_1.
r_{a2} = Internal resistance of valve V_2.
I = Anode current of each valve at balance ; i.e., with no input and with $I_m = 0$.
I_m = Current through the meter with an input E_{IN}.
I_1 = Anode current of valve V_1 with an input E_{IN}.
E_{IN} = Unidirectional input voltage, applied to make the input grid negative.
E_{B1} = Bias voltage of V_1 with no input.
E_{B2} = Bias voltage of V_2 with no input.
E'_{B1} = Bias voltage of V_1 with an input E_{IN}.
E'_{B2} = Bias voltage of V_2 with an input E_{IN}.

If the two valves V_1 and V_2 in Fig. 1 are first balanced with no input, then I_m is zero. If the resistance R_m is made infinite in value, the application of an input voltage E_{IN} will have no effect at all on the operating conditions of the valve V_2.

With R_m infinite, if E_{IN} is a negative input voltage then the potential of the cathode of V_1, with respect to negative h.t., will be lowered by a voltage equal to $E_{IN}\{(g_1R/(1 + g_1R)\}$, where g_1 is the effective mutual conductance of V_1 with an anode-cathode load of resistance R ; i.e.,

$$g_1 = g_{m1}\frac{r_{a1}}{r_{a1} + R}$$

Hence the potential difference between the cathodes of the two valves V_1 and V_2 will be equal to,

$$E_{IN}\frac{g_1R}{1 + g_1R}$$

If $g_1R \gg 1$ then this voltage $\approx E_{IN}$.

The change in potential of the cathode of V_1 corresponds to the change in valve operating conditions from the point O to the point X in Fig. 5. The line OX has a slope corresponding to a resistance value R.

Finite Meter Current

If now, the resistance R_m connected between the two cathodes is made finite in value, the meter current I_m flows as shown in Fig. 1 and the operating conditions of V_1 will now correspond to the change OY in Fig. 5.

Under the operating condition represented by the point " O ", the valve V_1 has an anode current I with an anode voltage $(V - IR)$ and a bias voltage E_{B1}. Under the conditions represented by the point " Y " the valve V_1 has an anode current of I_1 with an anode voltage $(V - IR) + \triangle E_{A1}$ and a bias voltage E'_{B1}.

The change OY is taken as the resultant of the two changes OZ and ZY. This means the anode current is assumed to change first from I to $(I_1 - \triangle I_1)$ with a change of bias from E_{B1} to E'_{B1} with a constant anode voltage $(V - IR)$; and then to change from $(I_1 - \triangle I_1)$ to I_1 with a constant bias E'_{B1} and a change in anode voltage from $(V - IR)$ to $(V - IR) + \triangle E_{A1}$.

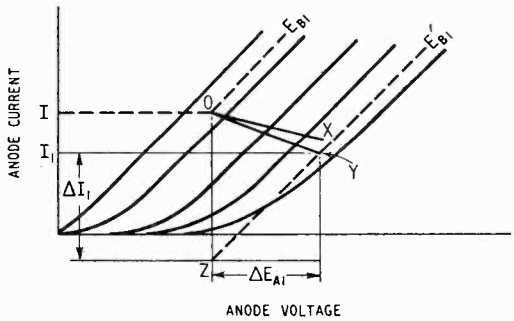

Fig. 5. *Typical curves illustrating the mode of operation.*

For Valve 1, we have :

With no input, bias $E_{B1} = E_1 - IR$

With input E_{IN}, bias $E'_{B1} = E_1 - E_{IN} - R(I_1 + I_m)$

Thus $E'_{B1} - E_{B1} = - E_{IN} - R(I_1 + I_m - I)$

The change in anode-cathode volts with input $E_{IN} = \triangle E_{A1}$

And $\triangle E_{A1} = \{V - R(I_1 + I_m)\} - (V - IR)$
$= R(I - I_1 - I_m)$

The change in anode current due to this is $\triangle I_1$, as shown in Fig. 5.

$$\text{And } \triangle I_1 = \frac{R(I - I_1 - I_m)}{r_{a1}} \quad \ldots \quad \ldots \quad \ldots (1)$$

The change in anode current due to the change in bias is $\triangle I_1 + I - I_1$ as also shown in Fig. 5.

And $\triangle I_1 + I - I_1 = -g_{m1}(E'_{B1} - E_{B1})$
$= -g_{m1}(-E_{IN} - I_1R$
$I_mR + IR)$

$$\therefore\ I_1(1 + g_{m1}R) - \triangle I_1 = I(1 + g_{m1}R) - g_{m1}E_{IN} - g_{m1}RI_m \quad \ldots \quad \ldots \quad \ldots (2)$$

Repeating for Valve 2 gives :—

$$\triangle I_2 = \frac{R(I - I_2 + I_m)}{r_{a2}} \quad \ldots \quad \ldots \quad \ldots (3)$$

$$I_2(1 + g_{m2}R) - \triangle I_2 = I(1 + g_{m2}R) + g_{m2}RI_m \quad \ldots \quad \ldots \quad \ldots \quad \ldots \quad \ldots (4)$$

Equations (1) and (2) give :—

$$I_1 - \frac{R(I - I_1 - I_m)}{r_{a1}(1 + g_{m1}R)} = I - \frac{1}{(1 + g_{m1}R)}(g_{m1}E_{IN} + g_{m1}RI_m)$$

Hence $I_1\left\{1 + \frac{R}{r_{a1}(1 + g_{m1}R)}\right\} = I\left\{1 + \frac{R}{r_{a1}(1 + g_{m1}R)}\right\} - \frac{1}{1 + g_{m1}R}\left\{g_{m1}E_{IN} + g_{m1}RI_m + \frac{R}{r_{a1}}I_m\right\}$

Let $1 + \frac{R}{r_{a1}(1 + g_{m1}R)} = \frac{1}{A_1}$ .. .. (5)

Then $I_1 = I - \frac{A_1}{1 + g_{m1}R}\left\{g_{m1}E_{IN} + g_{m1}RI_m + \frac{R}{r_{a1}}I_m\right\}$ .. .. (6)

Similarly equations (3) and (4) give :—

$$I_2 = I + \frac{A_2}{1 + g_{m2}R}\left\{g_{m2}RI_m + \frac{R}{r_{a2}}I_m\right\} \quad .. \quad (7)$$

where $\frac{1}{A_2} = 1 + \frac{R}{r_{a2}(1 + g_{m2}R)}$ .. .. (8)

Equations (6) and (7) give :—

$$I_2 - I_1 = \frac{A_1 g_{m1} E_{IN}}{1 + g_{m1}R} + \frac{A_1}{1 + g_{m1}R}\left(g_{m1}RI_m + \frac{R}{r_{a1}}I_m\right) + \frac{A_2}{1 + g_{m2}R}\left(g_{m2}RI_m + \frac{R}{r_{a2}}I_m\right) \quad .. \quad (9)$$

In the network joining the two cathodes in Fig. 1 :

$$I_m R_m + R(I_1 + I_m) = R(I_2 - I_m)$$

Hence $I_2 - I_1 = \frac{I_m(R_m + 2R)}{R}$ .. (10)

Equations (9) and (10) then give :

$$I_m\left\{R_m + R - \frac{A_1 R}{1 + g_{m1}R}\left(g_{m1}R + \frac{R}{r_{a1}}\right) + R - \frac{A_2 R}{1 + g_{m2}R}\left(g_{m2}R + \frac{R}{r_{a2}}\right)\right\} = \frac{A_1 g_{m1} E_{IN} R}{1 + g_{m1}R} \quad .. \quad .. \quad .. \quad (11)$$

Substituting for A_1 and A_2 from equations (5) and (8) respectively and simplifying gives :—

$$I_m\left\{R_m + \frac{R \cdot r_{a1}}{R + r_{a1}(1 + g_{m1}R)} + \frac{R \cdot r_{a2}}{R + r_{a2}(1 + g_{m2}R)}\right\} = \frac{E_{IN}\, g_{m1} R r_{a1}}{R + r_{a1}(1 + g_{m1}R)} \quad .. \quad .. \quad .. \quad (12)$$

Let r_{a1} and R in parallel $= R'_1 = \frac{r_{a1} R}{R + r_{a1}}$

and r_{a2} and R in parallel $= R'_2 = \frac{r_{a2} R}{R + r_{a2}}$

then from (12) $I_m\left\{R_m + \frac{R'_1}{1 + g_m R'_1} + \frac{R'_2}{1 + g_{m2}R'_2}\right\} = \frac{g_{m1}R'_1}{1 + g_{m1}R'_1} \cdot E_{IN}$.

If $g_{m1}R'_1 \approx g_{m2}R'_2 \gg 1$

then $I_m = \frac{E_{IN}}{R_m + \frac{1}{g_{m1}} + \frac{1}{g_{m2}}}$ .. .. 13)

APPENDIX II

In the analysis of the circuit shown in Fig. 2 the following symbols are used :—

H.T. voltage $= V$

$E = kV$ where k is a constant.

r_{a1}, r_{a2}, g_{m1} and g_{m2} are as defined in Appendix 1.

$g_1 = g_{m1}\frac{r_{a1}}{r_{a1} + R_{L1} + R_1}$

$g_2 = g_{m2}\frac{r_{a2}}{r_{a2} + R_{L2} + R_2}$

$\mu_1 = g_{m1} r_{a1}$

$\mu_2 = g_{m2} r_{a2}$

I_1 = anode current of valve V_1 with an h.t. voltage V.

$I_1 + \delta I_1$ = anode current of valve V_1 with an h.t. voltage $V + \Delta V$).

R_{L1} = anode resistance of V_1.

R_{L2} = anode resistance of V_2.

R_1 = cathode resistance of V_1.

R_2 = cathode resistance of V_2.

The change from the conditions represented by point " O " to those represented by point " P " in Fig. 6 is the change in the valve V_1 as the h.t. voltage is altered from V to $V + \Delta V$ with a consequent change in anode current from I_1 to $I_1 + \delta I_1$. The bias voltage of V_1 changes from E_{B1} to E'_{B1} at the same time.

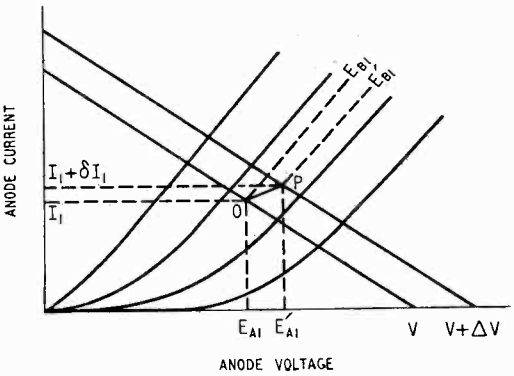

Fig. 6. *The change in valve conditions due to an h.t. voltage change is shown.*

Then as before $E_{B1} = E - I_1 R_1$

and $E'_{B1} = E + \Delta E - R_1(I_1 + \delta I_1)$

Also $E_{A1} = V - I_1(R_{L1} + R_1)$

and $E'_{A1} = V + \Delta V - (I_1 + \delta I_1)(R_{L1} + R_1)$

and the change in anode current due to the change $E'_{A1} - E_{A1}$ is

$$\frac{E'_{A1} - E_{A1}}{r_{a1} + R_{L1} + R_1} \quad .. \quad .. \quad .. \quad .. \quad (14)$$

and the change in anode current due to the change in bias $E_{B1} - E'_{B1}$ is,

$$-g_1(E_{B1} - E'_{B1}) \quad .. \quad .. \quad .. \quad (15)$$

Hence (14) and (15) give,

$$\delta I_1 = \frac{E'_{A1} - E_{A1}}{r_{a1} + R_{L1} + R_1} - g_1(E_{B1} - E'_{B1})$$

Substituting for E'_{A1}, E_{A1}, E'_{B1}, E_{B1} and simplifying gives :

$$\delta I_1 = \frac{\triangle V + \mu_1 \triangle E}{r_{a1} + 2R_{L1} + R_1 (2 + \mu_1)} \quad \ldots \quad \ldots (16)$$

∴ Change of voltage across R_1 when the h.t. voltage changes from V to $(V + \triangle V)$

$$= \frac{R_1(\triangle V + \mu_1 \triangle E)}{r_{a1} + 2R_{L1} + R_1 (2 + \mu_1)}$$

$$= \frac{\triangle V}{\dfrac{r_{a1} + 2R_{L1}}{R_1 (1 + k\mu_1)} + \dfrac{2 + \mu_1}{1 + k\mu_1}}$$

$$\approx \frac{\triangle V}{\dfrac{r_{a1} + 2R_{L1}}{R_1 (1 + k\mu_1)} + \dfrac{1}{k}}$$

and change in voltage across R_2

$$\approx \frac{\triangle V}{\dfrac{r_{a2} + 2R_{L2}}{R_2 (1 + k\mu_2)} + \dfrac{1}{k}}$$

CORRESPONDENCE

Standard Terms and Abbreviations

Mr. Hart, in the May issue, joins in advocating the adoption of "K" as the abbreviation for "kilo." The lower case "k" is adopted by C.C.I. and by most, if not all, the standardization committees of European countries, and it must be pointed out that to them the metric system is a matter of daily life and they are unlikely to change their habits. The use of "K" derives from a false analogy with "M" and "D" for mega and deka, and where no confusion can be caused I would advocate the use of the lower case "m" even for mega, in mc/s, but not in MW. The object of using abbreviations is economy, and in typing, the capital letters involve three operations, compared with the single operation for the lower case letters.

The use of "m" in place of "μ," as in "mF," although apparently illogical, is dictated by a factor which both you and your correspondents have overlooked : most typewriters cannot produce "μ." The result is that the engineer who wishes to avoid lengthy corrections of perhaps half a dozen copies chooses a form which can be followed by the typist. If he doesn't, the eccentric 'uF' sooner or later creeps in. This limitation applies also to spelling : your contributors must run the gauntlet past their typist, the editor, and the printer. The typist, armed with Pitman's dictionary, will insist, for example, on "standardise" ; until recently I believe this was also your practice. The engineer has very little hope of finding his own self-consistent scheme reproduced in the final copy.

As a basis for a self-consistent usage, I would draw your attention to "Rules for Compositors and Readers at the University Press, Oxford," which used to cost 2s. 6d. This gives for example an unambiguous ruling on whether to write 'a f.m.' or 'an f.m.' ; "print *a*, not *an*, before contractions beginning with a consonant."

There are two very useful prefixes, one of which is fairly widely used on the Continent, which deserve mention. They are Giga = 10^9 and nano = 10^{-9}. I have not seen any references to a 10 Gc/s radar, although it is an attractive form, but Dutch and Swedish circuits often contain 50 nF capacitors, in place of the more cumbersome (especially in speech) 0.05 μF, and even 50 000 pF. I would urge their adoption before kMc/s and kpF are established.

H. JEFFERSON.

Stockholm, Sweden.

SIR,—This discussion is very interesting, and I hope others will contribute their views. Using amp for ampere is an old fad of mine ; everyone says it, so why not write it ? But I cannot work up much enthusiasm for altering k to K, although it would be slightly more consistent. For further consistency we might then be required to write m.K.s. system. Is it also proposed to alter h to H (as in ha, hectare) ? I hope no one advocates D (deca), owing to possible confusion with d (deci).

My own solution of the kilocycle problem is this. Make c the abbreviation for cycles per second ; then kc (or Kc if it is agreed) is the correct abbreviation for kilocycles per second, and similarly for Mc. The occasions for using cycles, as distinct from cycles per second, are comparatively rare, usually in connection with loss per cycle, and I cannot then remember seeing it abbreviated to c. It may still be objected that to speak, as we do, of kilocycles without the per second, is inaccurate. Then go a stage further. Define cycles as alternations per second, and our loose speech becomes correct. This second step, however, appears pedantic, as most unprepared speech *is* inaccurate. But the present written practice seems indefensible. In the aggregate we spend hours of otherwise useful lives, and waste reams of paper, writing, typing and printing repetitions of an unnecessary /s. The position is similar to the absurd one which would arise if we were permitted C for coulomb (why not coul ?), but not A for amp ; then C/s would appear *ad nauseam* in all our written work.

A tenable alternative for cycles per second is hertz, except that its abbreviation H would be the same as that for henry. Not that I favour henry, because I am never sure whether its plural should be henrys or henries, and because it cannot be reversed to give the reciprocal unit like mho and daraf.

Mr. Hart's rule for upper or lower case in abbreviations results, at the beginning of sentences, in expressions like "U.h.f. techniques . . . ." Perhaps he advocates such hybrids ? But the rule fails for units, since in opposition to Mr. Odell, I maintain that whilst Ampère and Bell are proper names, amp and bel are common nouns and not entitled to capitals. As regards db or dB, I prefer the former because it is easier to write !

Is it not time that the convenient nano (n, 10^{-9}) and pico (p, 10^{-12}) were officially recognized ? But we should not introduce permanent symbols unless they are definitely needed. With so much of the alphabet allocated to units and quantities, it becomes increasingly difficult to find a spare symbol when one is wanted. And we should take care not to clash with other users. Thus it is fortunate that the picohenry is too small a unit for frequent use, since I am assured that pH means something quite different.

T.C & M. Co., Ltd.,
Greenwich, S.E.10. A. L. MEYERS.

Signal-Noise Ratio in Radar

SIR,—In your March issue Mr. de Walden criticizes my paper on "Signal-Noise Ratio in Radar" His main argument is that in a radar display the presence of a signal is detected by observation of a

bodily displacement of part of the noise pattern from the ideal line of scanning, and not by observation of changes of brightness along this line.

To justify his argument and to prove the fallacy of my assumptions, Mr. de Walden gives the following example.—"Suppose that the electron beam is defocused into a uniformly illuminated disc of diameter d and that the noise level is negligible. In the absence of signals the scanned pattern will then appear as a uniformly bright band of height d. If the criterion for detecting signals were a change of brightness along the ideal scanning line, which is the middle line of this band, any signals of amplitude smaller than $d/2$ would not be detected, which is obviously not the case."

This argument is based on two fundamental fallacies. First, as Dr. Espley pointed out spontaneously to me, if the electron beam is defocused into a uniformly-illuminated disc of diameter d, the scanned pattern will not appear as a uniformly bright band of height d, since points on the axis of symmetry of the scanned pattern are scanned longer than those away from this axis. The brilliance will decrease progressively from the axis outwards. This is well known to television engineers.

Secondly, in the presence of noise, this phenomenon is accentuated, and one cannot any more speak of upper or lower edges of the scanned pattern. I believe I explained this very clearly in my paper.

If Mr. de Walden's letter were confined to its two last paragraphs I would approve his points, but his main criticism does not seem justified to me.

I would like to take advantage of this letter to add some comments to my paper.

The aim of the paper was to give an example of the application of statistics to radio problems. The limitations are those of theoretical papers where emphasis is made on the principle only and where, for simplicity, all modifications introduced by practical and experimental considerations are not considered.

In particular, I took no account of what happens during detection. After detection the noise is positive only and cannot take negative values. Even if the d.c. component is suppressed, the negative deflections are bounded. This is not expressed by a Gaussian curve, which has an infinite tail on each side of the peak. The Gaussian law should be replaced by Rayleigh's law whose equation is (I am indebted to Z. Jelonek for comments on this point),

$$p(z) = \frac{2z}{\alpha_n^2} e^{-z^2/\alpha_n^2} \quad (z > 0)$$

the notation being the same as that used in my paper. The fact that the noise can only be positive is expressed by the introduction of Z in the right-hand side. For very small amplitudes of noise the Gaussian and Rayleigh laws are different; for large amplitudes the difference is very small. However, both types of curves have a maximum and the method explained in my paper applies to both.

Wembley, Middx. M. LEVY.

BOOK REVIEW

Vacuum Tubes

By KARL R. SPANGENBERG. Pp. 860 + xvii, with 500 illustrations. McGraw-Hill Publishing Co., Aldwych House, London, W.C.2. Price 45s. (in U.K.).

This important book is designed to give a comprehensive account of vacuum tubes and the physical laws on which their behaviour depends. It contains a splendid collection of potential-distribution diagrams, nomograms and design charts pertaining to electron optics, thermionic receiving valves and the more recent developments, such as klystrons and magnetron oscillators. The author aims to explain the internal operation of valves, and hence little attention is devoted to external circuits; a similar object was proclaimed by Dow, in his well-known book "Fundamentals of Engineering Electronics." The natural topics of discussion in the early chapters are therefore Poisson's and Laplace's equations, potential fields, conformal representation, and then the laws of electron motion, leading up to an exposition of triode theory. The analysis of triode fields is particularly well done, and even if the mathematics be deemed moderately difficult, it is of the standard the subject matter requires.

The section on beam tetrodes is not very satisfactory, probably because no very satisfying theory of their behaviour yet exists. The treatment of pentodes is excellent, although perhaps too much attention is given to the problem of evaluating the overall electrostatic amplification factor. Noise is probably adequately discussed—the photocurrent yielding a given noise is correctly given on p. 318, so that the value given on p. 700 is in error.

A large and excellent section of the book is devoted to electron optics—mainly paraxial theory—and cathode-ray tubes. The bringing together of charts for optical characteristics of lens systems, and the P-Q curves for various lenses is particularly welcome. The chapter on magnetic lenses could be amplified by a description of Goddard and Klemperer's valuable computational method of electron-ray tracing.

The treatment of the fundamental theory of transit-time effects appears to be sound. The reviewer suggests however that the logical starting point is the equation of continuity for current flow, because the specifically Maxwellian postulate that displacement current contributes fully to the magnetic field is ignored, except in such advanced papers as that by Gabor "On the Conversion of Energy in Electronic Devices."[1] In the chapter on "Special Tubes" the description given of the operation of the Iconoscope is well below the level set by the rest of the book, and it is surprising to read that "image iconoscopes have not found great use." However, the book is remarkably free from errors; the main demerit throughout is the inadequate tribute to many workers who have added notably to electronic science—few readers, for example, would gather that Benham has been an outstanding pioneer in the study of transit-time effects. Apart from this, the book is outstanding in its merits as a comprehensive exposition of vacuum-tube theory.

S. R.

[1] *J. Instn elect. Engrs*, Vol. 91, Part III, No. 15, Sept. 1944, p. 128.

WIRELESS PATENTS

A Summary of Recently Accepted Specifications

The following abstracts are prepared, with the permission of the Controller of H.M. Stationary Office, from Specifications obtainable at the Patent Office, 25, Southampton Buildings, London, W.C.2, price 1/- each.

DIRECTIONAL AND NAVIGATIONAL SYSTEMS

590 460.—Method of co-ordinating the timing of two pulsed beacon-stations for marking-out a given navigational course.

Standard Telephones and Cables Ltd. (assignees of E. Labin). Convention date (U.S.A.) 28th June, 1941.

590 461.—Radio beacon system in which a frequency-modulated pattern is rotated relatively to a "reference" direction.

Bendix Aviation Corporation. Convention date (U.S.A.) 16th July, 1942.

590 469.—Radiolocation system in which the aerial tuning is cyclically varied in order to offset the effect of enemy jamming.

Standard Telephones and Cables Ltd. (assignees of R. B. Hoffman). Convention date (U.S.A.) 28th November, 1942.

590 470.—High-speed switching-device, suitable for use in radiolocation, in which resonant elements are controlled by an electric discharge to open or close the aerial circuits.

Marconi's W.T. Co. Ltd. (assignees of M. R. Richmond). Convention date (U.S.A.) 25th February, 1943.

590 489.—Radiolocation system, adapted to observe both target and projectile, and to detonate the latter when it comes into close proximity with the former.

Standard Telephones and Cables Ltd. (assignees of E. M. Deloraine). Convention date (U.S.A) 22nd August, 1942.

590 491.—Blind-landing system in which an elevated aerial, fed with sideband energy, is arranged to radiate lobes which form a null zone along the gliding path, whilst a second aerial radiates the modulated carrier-wave to give an equi-signal response along that path.

Standard Telephones and Cables Ltd. (assignees of A. Alford). Convention date (U.S.A.) 7th May, 1942.

590 504.—Rotary aerial system and time-base circuit for giving a visual plan-indication of objects within the range of a radiolocation set.

Western Electric Co. Incorp. Convention date (U.S.A.) 20th December, 1941.

590 620.—Navigational system in which radiolocation equipment carried on an aircraft triggers beacon transmitters at the airport to radiate a pulsed approach-track and a vertical glide-path.

Standard Telephones and Cables Ltd. (assignees of N. Marchand). Convention date (U.S.A.) 6th September, 1943.

590 701.—Radiolocation system in which the pulse-repetition frequency is varied in order to convey telegraphic or telephonic signals.

Standard Telephones and Cables Ltd. (assignees of E. Labin; D. D. Greig and A. M. Levine). Convention date (U.S.A.) 6th November, 1943.

590 711.—Automatic gain-control system for periodically adjusting the sensitivity of a receiver of pulsed signals, say in connection with radiolocation equipment.

Hazeltine Corpn. (assignees of R. B. J. Brunn). Convention date (U.S.A.) 19th February, 1944.

590 772.—Directive aerial system in which a central unit or array, fed with current of constant phase, is flanked by side units, in line with each other and energized by currents of graded phase.

Marconi's W.T. Co. Ltd. and V. J. Cooper. Application date 18th June, 1943.

590 944.—Radiolocation system in which an electron camera having a charge-storage screen is interposed between a primary and final c.r. indicator, in order to increase the signal-to-noise ratio of the received echoes.

Western Electric Co. Inc. Convention date (U.S.A.) 5th October, 1943.

RECEIVING CIRCUITS AND APPARATUS

590 539.—Radio chassis-assembly comprising a set of substantially-flat and flanged interlocking units, arranged in box-like fashion.

Standard Telephones and Cables Ltd. (assignees of S. H. M. Dodington). Convention date (U.S.A.) 11th December, 1943.

590 910.—Construction of a cabinet for a radio receiver, comprising two end-pieces connected together by a baffle-board, and covered by a single moulded top-piece.

Philips Lamps Ltd. and C. L. Richards. Application date 12th January, 1945.

TRANSMITTING CIRCUITS AND APPARATUS

590 302.—Waveguide in which slots are cut in the thickness of the walls in order to filter-out the transverse-electric from the transverse-magnetic type of wave.

Western Electric Co., Inc., Convention date (U.S.A.) 28th April, 1944.

590 473.—Tuned tank-circuit, particularly for an amplifier, comprising a transmission-line element, of suitable dimensions, which is closed on itself to eliminate end-effects.

Marconi's W.T. Co. Ltd. (assignees of W. van B. Roberts). Convention date (U.S.A.) 26th September, 1942.

590 651.—Waveguide terminating in a tapered section, formed with graded apertures, in order to dissipate power without radiation, or for impedance-matching purposes.

G. E. F. Fertel and C. S. Wright. Application date 3rd August, 1944.